A MOBILE FACILITY FOR MEASURING THE BACKSCATTERING AND BRIGHTNESS TEMPERATURE OF TERRAIN AT MICROWAVE FREQUENCIES

T.L. Oliver

The Ohio State University

ElectroScience Laboratory

(formerly Antenna Laboratory)
Department of Electrical Engineering
Columbus, Ohio 43212

REPORT 1903-6

Contract Number NSR-36-008-027
4 October 1968

National Aeronautics and Space Administration
Office of Grants and Research Contracts
Washington, D.C., 20546

NOTICES

When Government drawings, specifications, or other data are used for any purpose other than in connection with a definitely related Government procurement operation, the United States Government thereby incurs no responsibility nor any obligation whatsoever, and the fact that the Government may have formulated, furnished, or in any way supplied the said drawings, specifications, or other data, is not to be regarded by implication or otherwise as in any manner licensing the holder or any other person or corporation, or conveying any rights or permission to manufacture, use, or sell any patented invention that may in any way be related thereto.

The Government has the right to reproduce, use, and distribute this report for governmental purposes in accordance with the contract under which the report was produced. To protect the proprietary interests of the contractor and to avoid jeopardy of its obligations to the Government, the report may not be released for non-governmental use such as might constitute general publication without the express prior consent of The Ohio State University Research Foundation.

REPORT

by

THE OHIO STATE UNIVERSITY ELECTROSCIENCE LABORATORY
(Formerly Antenna Laboratory)
COLUMBUS, OHIO 43212

Sponsor	National Aeronatuics and Space Administration Office of Grants and Research Contracts Washington, D.C. 20546
Contract Number	NSR-36-008-027
Investigation of	Radar and Microwave Radiometric Techniques for Geoscience Experiments
Subject of Report	A Mobile Facility for Measuring the Backscattering and Brightness Temperature of Terrain at Microwave Frequencies
Submitted by	T.L. Oliver ElectroScience Laboratory Department of Electrical Engineering
Date	4 October 1968

The material contained in this report is also used as a thesis submitted to the Department of Electrical Engineering, The Ohio State University as partial fulfillment for the degree Master of Science.

ABSTRACT

The design and construction of a truck-mounted facility for measuring the backscattering and brightness temperature of terrain at microwave frequencies are discussed, including procedures for calibration and data reduction. Descriptions of the linearly polarized, c-w doppler radar systems, operated at 1.8, 10, 15 and 35 GHz, and the radiometer systems (10 and 35 GHZ) are also presented.

TABLE OF CONTENTS

CHAPTER I

INTRODUCTION

Recent interest in the response of microwave sensors (radar and radiometer) to natural surfaces has been greatly stimulated by the increased availability of imagery over areas of agricultural, geologic, hydrologic, and oceanographic significance. The potential of the radar as a remote sensor for earth science and resource studies has been summarized by Moore and Simonett.[1] For example, geological faults and lineaments have been located on radar imagery which were not visible on aerial photos;[2,3] in addition, simultaneously produced like-and cross-polarized radar imagery has added significantly to lithologic differentiations.[4] Because of its later development, the use of the imaging microwave radiometer as a remote sensor is as yet rather limited. Recently, however, the U.S. Coast Guard[5] has operated an imaging radiometer designed to detect targets, especially icebergs, against a seawater background. Also, NASA[6] has made radiometer observations of the Earth over a variety of geographical areas, including Ocean ice, Southwestern U.S. deserts, Midwest U.S. farmland, and storm and rain clouds over both land and water.

For the interpretation of this imagery and for the design of remote sensors, basic information about the terrain return characteristics of the surface is required. Furthermore, the determination of these basic surface characteristics in the microwave region can be made more effectively when data is available from both radar and radiometer

sensors,[7] because each output is determined by a different aspect of the complete bistatic scattering pattern of the surface; the backscatter is estimated by the radar while the brightness temperature (which is related to the albedo), is estimated by the radiometer.

To provide simultaneous data from combined radar and radiometer sensor outputs, the O.S.U. mobile radar-radiometer facility (see Fig.1) was constructed. The self-contained unit permits in situ measurements of the normalized backscattering cross section (per unit area) of terrain, $\sigma^o(\theta)$, and the brightness temperature of an antenna viewing the terrain, $T_{ant}(\theta)$, at microwave frequencies.

The purpose of this report is to describe the mobile facility and its operation, including methods for calibration and data reduction. Some examples of backscattering and brightness temperature data are also presented.

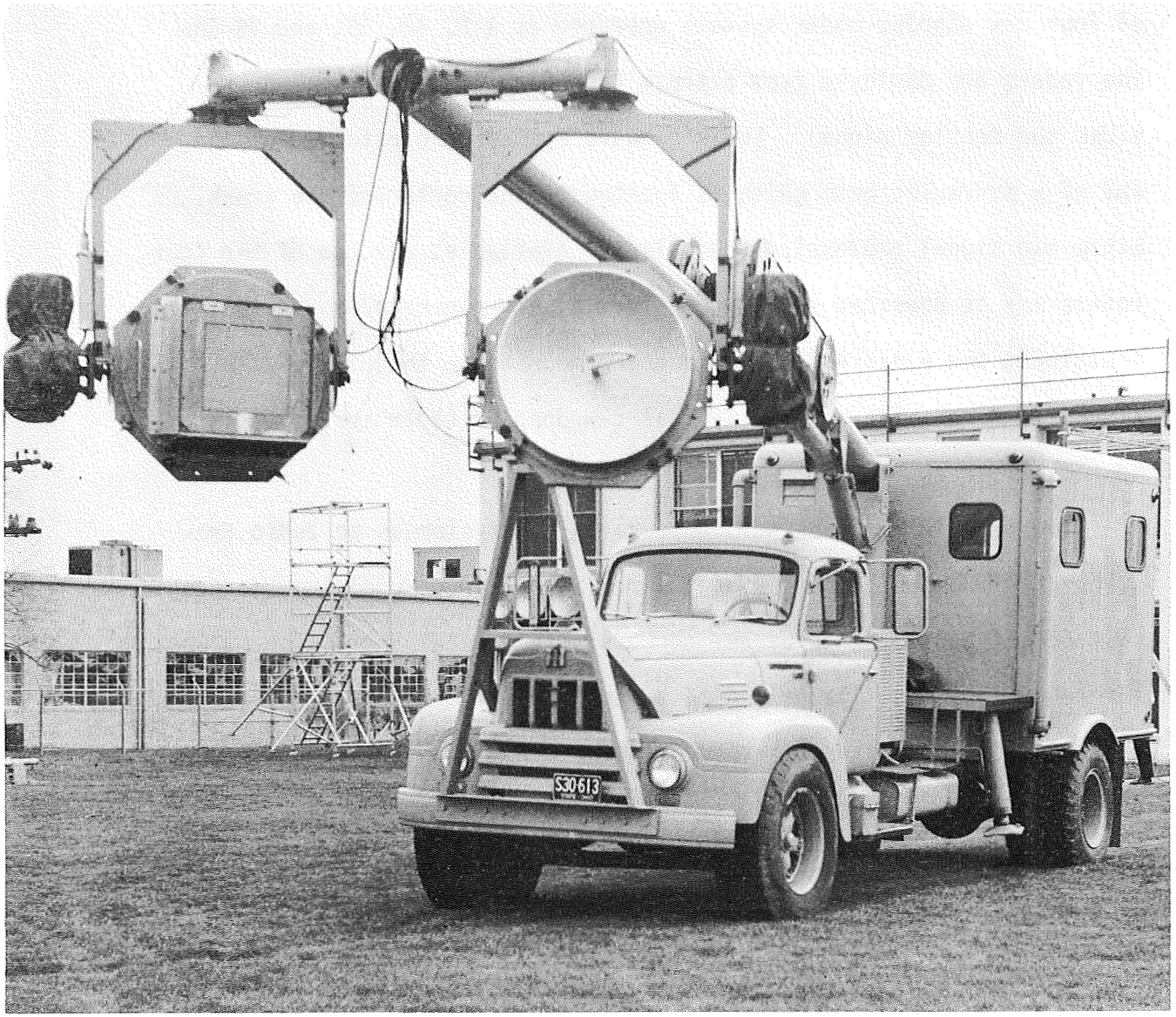

Fig. 1. The O.S.U. Mobile Radar-Radiometer Facility.

CHAPTER II

RADAR FACILITIES

The O.S.U. multi-frequency terrain-return radar facility consists of four c-w doppler radar systems operated at 1.8, 10, 15, and 35 GHz. The radars are deployed from a truck (see Fig. 1), whose motion provides the doppler signal. The microwave systems are attached at the end of a hydraulic boom which is located at the center of the truck. Since two signal processing channels are available, any two of the four radars may be operated simultaneously. A 5-Kw generator and a van containing the electronic equipment are mounted to the rear of the truck. A block diagram of a typical c-w doppler radar system is shown in Fig. 2.

The terrain return signal appears in the system as an audio frequency (narrow band) noise signal which is obtained by mixing the doppler shifted signal scattered by the terrain with a local oscillator. The reference local oscillator signal at the crystal mixer is supplied by a small amount of transmitter power. The doppler shift is obtained by driving the truck at a predetermined speed across the terrain. To insure that the frequency shift is within the preamplifier passband for each angle of incidence, the speed is calculated as follows:[8]

$$(1) \qquad v_t = \frac{\lambda \Delta f}{2 \sin\theta \cos\phi} \quad ,$$

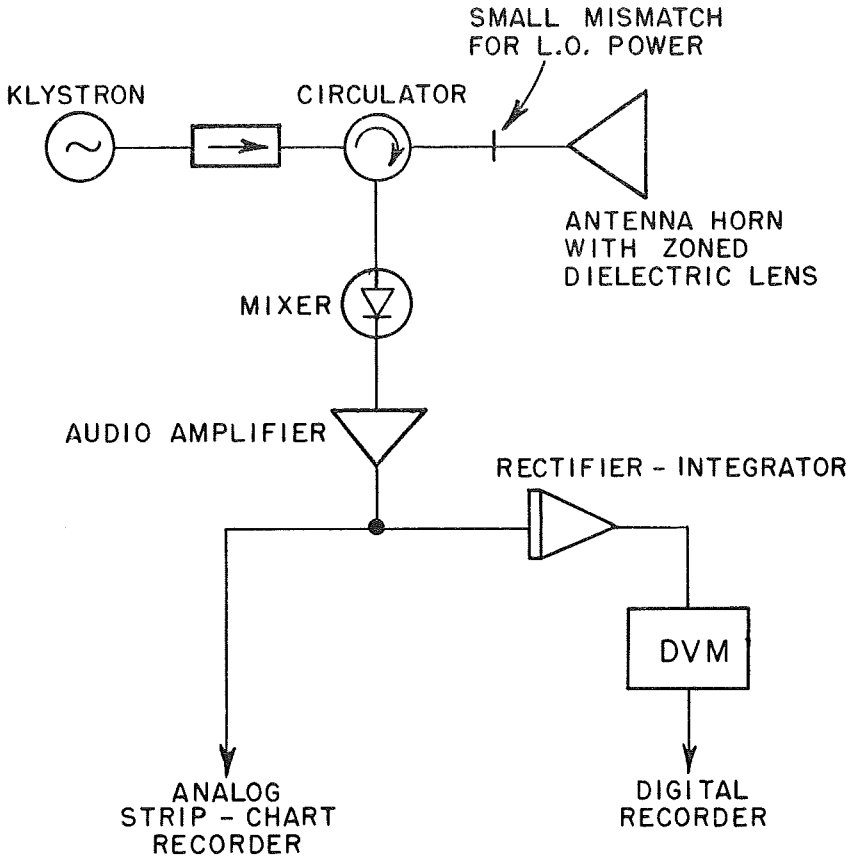

Fig. 2. Block diagram of a typical c-w doppler radar system.

where v_t - truck speed in meters/sec,

Δf = frequency shift in Hz,

λ = wavelength in meters,

θ = angle of incidence from normal,

ϕ = angle in horizontal plane between velocity vector of the truck and the direction in which the antenna is pointed (see Fig. 3).

Radar terrain return measurements are normally taken at incidence angles (from normal) of 20^o, 30^o, 40^o, 50^o, 60^o and 70^o, with the truck

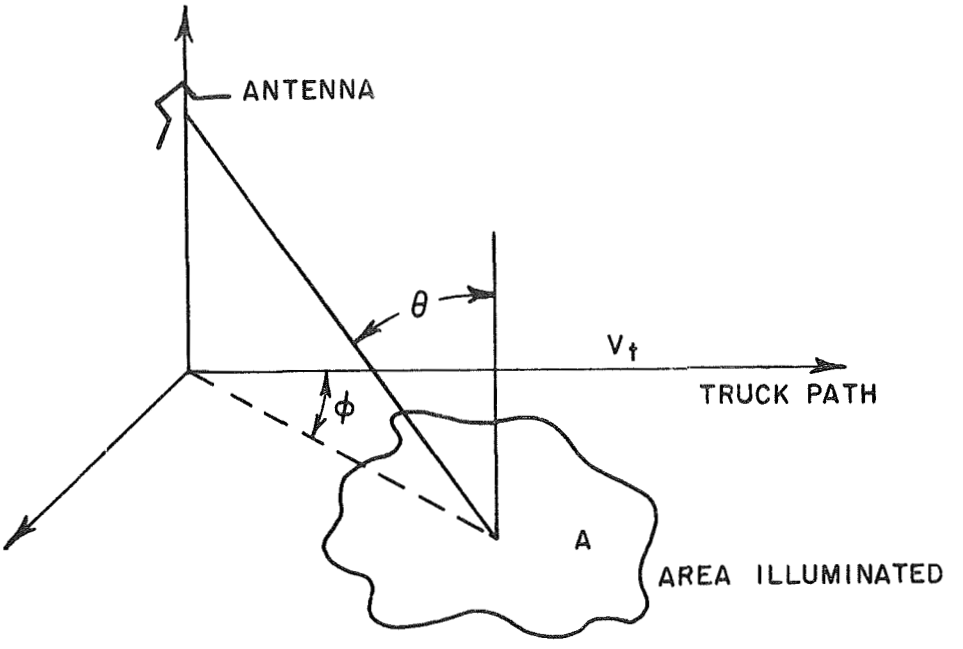

Fig. 3. Geometry for Eq. (1).

traveling in both forward and reverse directions. For near normal incidence angles, too much speed is required for safe operation, except on very smooth surfaces; near grazing, the target area definition is poor.

The purpose of the radar measurements is to determine the normalized backscattering parameters of the terrain $-\sigma^o_{jk}(\theta_i)$ or $\gamma_{jk}(\theta_i)$, where θ_i is the angle with respect to the surface normal. The governing parameter at microwave frequencies is actually the normalized bistatic scattering cross section (per unit surface area),[7] $\sigma^o_{jk}(i,s)$, where (see Fig. 4) the subscript j refers to the polarization of the incident

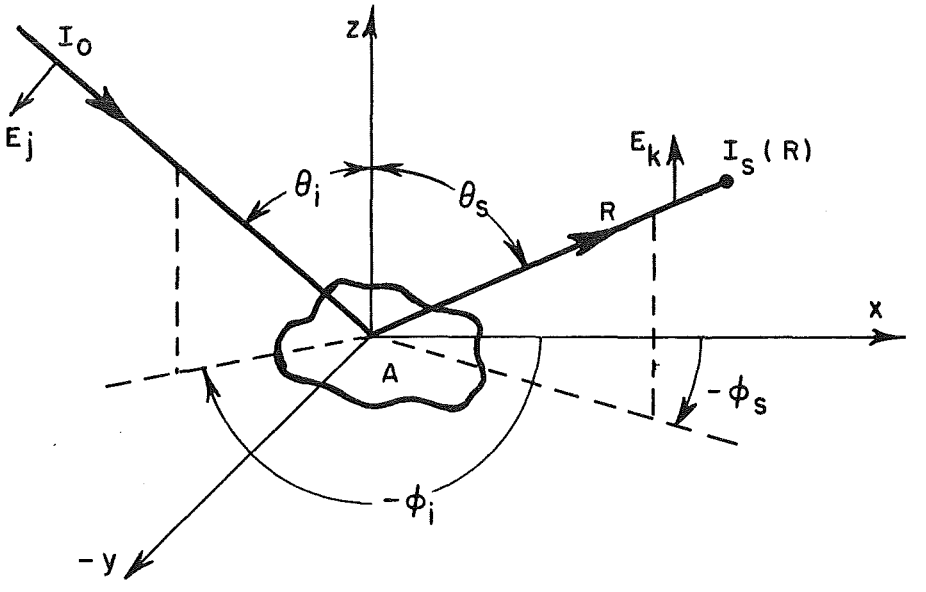

Fig. 4. Geometry of the scattering problem.

radiation on the surface of area A, and the subscript k designates that polarization component of the scattered signal which is accepted by the receiving antenna; i,s refer to the angles (θ_i,ϕ_i) and (θ_s,ϕ_s) defining the propagation directions of the incident and scattered radiation.

Operationally, the bistatic cross section is defined by considering an area A which is illuminated by a plane wave of power density I_o (watts/m^2), and which produces a scattered intensity I_s at a distance R. The normalized bistatic scattering cross section $\sigma^o{}_{jk}(i,s)$ is then defined by the equation[9]

$$(2) \qquad \sigma^o_{jk}(i,s) = \frac{4\pi R^2 I_s}{A I_o} = \sigma^o_{kj}(s,i) \qquad \text{(reciprocity theorem)},$$

where this normalized bistatic cross section, σ^o, is related to the conventional radar cross section, σ, by $\sigma^o = \sigma/A$. In terms of this parameter, the normalized radar backscattering cross section is $\sigma^o_{jk}(i,i)$ or just $\sigma^o_{jk}(\theta_i)$; the particular polarization states used in this report are designated by the following notation:

	Transmitted wave	Received scattered wave
σ^o_{VV}	vertically polarized	vertically polarized
σ^o_{VH}	vertically polarized	horizontally polarized
σ^o_{HH}	horizontally polarized	horizontally polarized
σ^o_{HV}	horizontally polarized	vertically polarized

The words "vertical polarized" refer to a wave with its electric vector in the plane of the incidence; the words "horizontal polarized" refer to a wave with its electric vector in the plane of the surface.

To work with a parameter which is independent of the illuminated area of the terrain, the bistatic radar return parameter per unit "projected" area, γ, is introduced by the relation

$$(3) \qquad \gamma_{jk}(i,s) = \frac{\sigma^o_{jk}(i,s)}{\cos\theta_i} = \frac{4\pi R^2 I_s}{I_o(A \cos\theta_i)} \quad .$$

Once again, the parameter of concern here is the backscattering component $\gamma_{jk}(i,i)$ or $\gamma_{jk}(\theta_i) = \sigma^o(\theta_i)/\cos\theta_i$. The reciprocity condition satisfied by the γ's is[7] $\gamma_{jk}(i,s) \cos\theta_i = \gamma_{kj}(s,i) \cos\theta_s$.

In the actual system described here, the resolved area at normal incidence (spot size), A_i, which is the area perpendicular to the incident beam at the range R (nominal operating range is 20'), is given by

$$(4) \qquad A_i = \pi R^2 \tan^2(\theta_{HP}/2)$$

$$= 400\pi \tan^2(\theta_{HP}/2) \quad \text{(sq. ft.)},$$

where θ_{HP} is the measured half-power antenna beamwidth at 20 feet. The spot sizes are given in Table I. To remove the statistical fluctuations in the return parameters, averaging is accomplished by driving the truck a distance of 100 to 200 feet along the terrain and integrating the return over many independent illuminated spots.

A. Systems

1. Microwave

The microwave transmitting and receiving network for each frequency is contained in a portable enclosure designed for easy attachment to and removal from the boom of the truck (see Fig. 5). Either horizontal, vertical, or any linear polarization can be used at each of the four frequencies. The S, K_u and K_a-band radars detect only a scattered signal of the transmitted polarizarion. The X-band radar receives a scattered signal of the transmitted polarization and also the cross-polarized component.

The microwave circuit block diagrams are shown in Figs. 6, 7, 8, and 9. The high isolation between the transmitter and receiver ports of the circulators necessitated the insertion of an iris at the antenna

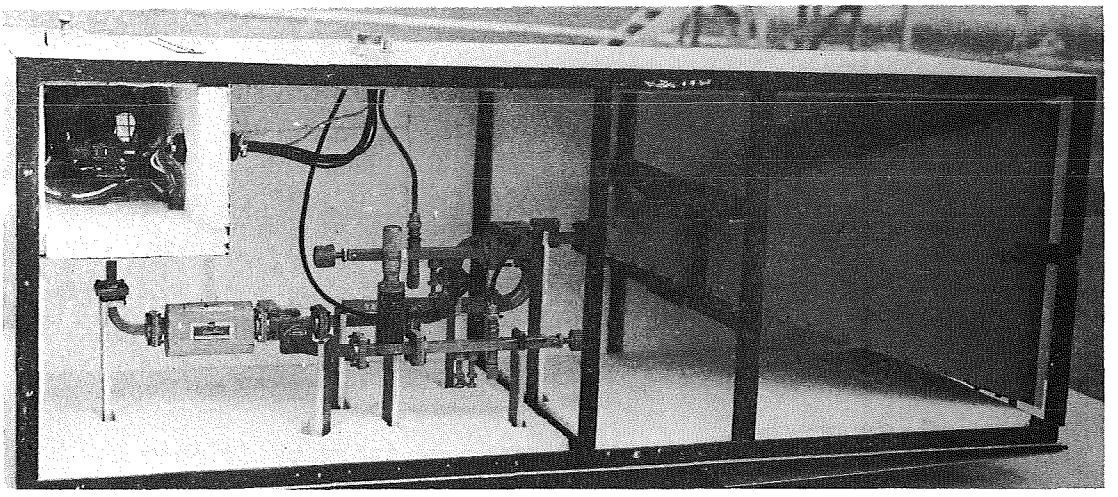

Fig. 5. K_u-band radar enclosure.

terminals of the circulator to provide the required l.o. power level at the mixer (see note on selection of l.o. power levels below). The microwave radar system specifications are presented in Table I.

The antennas used in the X-, K_u-, and K_a-band systems are high-gain pyramidal horns with zoned dielectric lenses.[10] These lenses give an optimum pattern at the operating range of 20 feet. The S-band antenna is a 3'-diameter parabolic reflector, which was slightly defocussed to obtain a better approximation to a plane wave at the operating range of 20 feet than would be given by a standard design. The radar antenna power patterns (presented in Appendix I) were measured at this operating range of 20 feet.

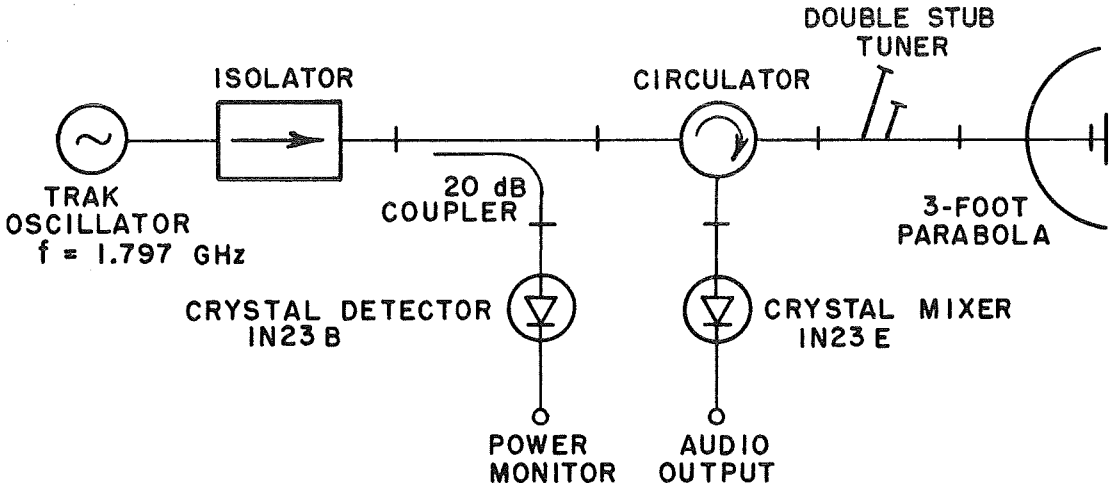

Fig. 6. S-band radar microwave circuit (λ=16.6 cm).

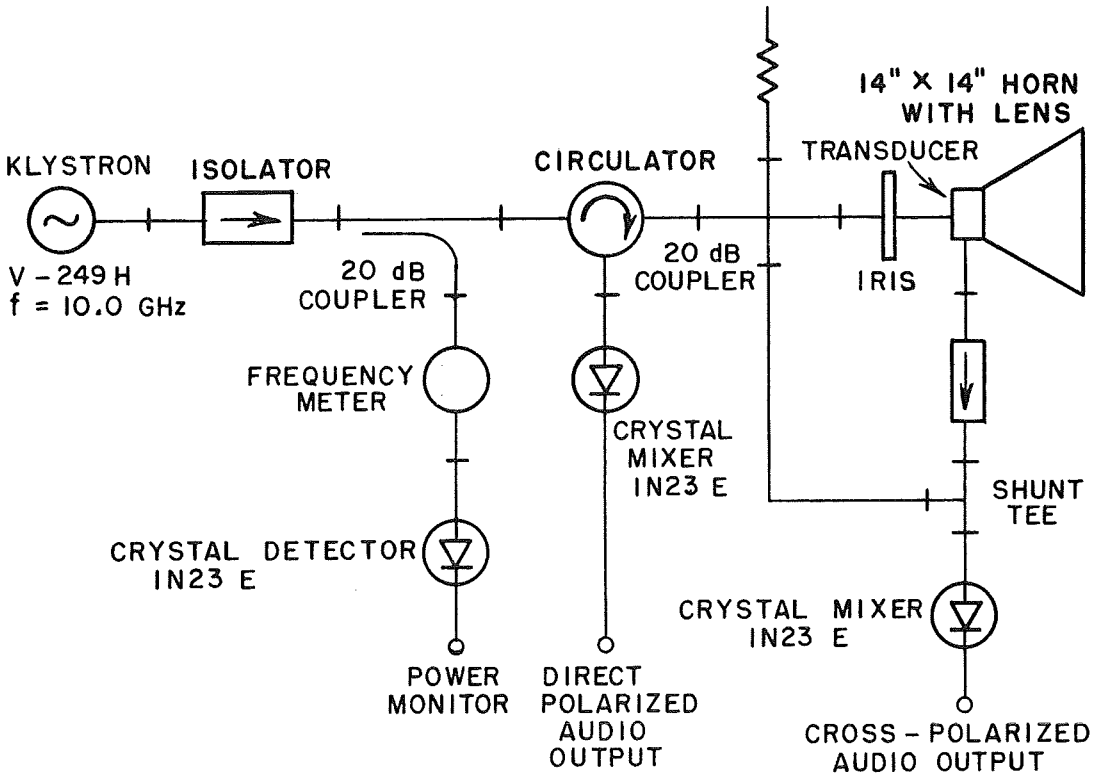

Fig. 7. X-band radar microwave circuit (λ=3.0 cm).

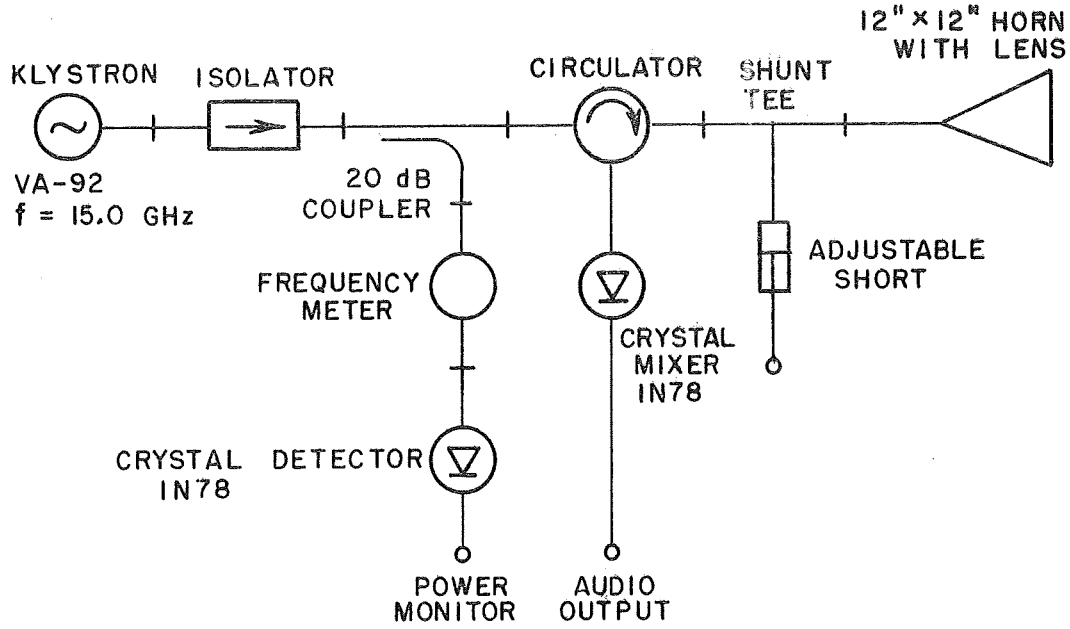

Fig. 8. K_u-band radar microwave circuit (λ=2.0 cm).

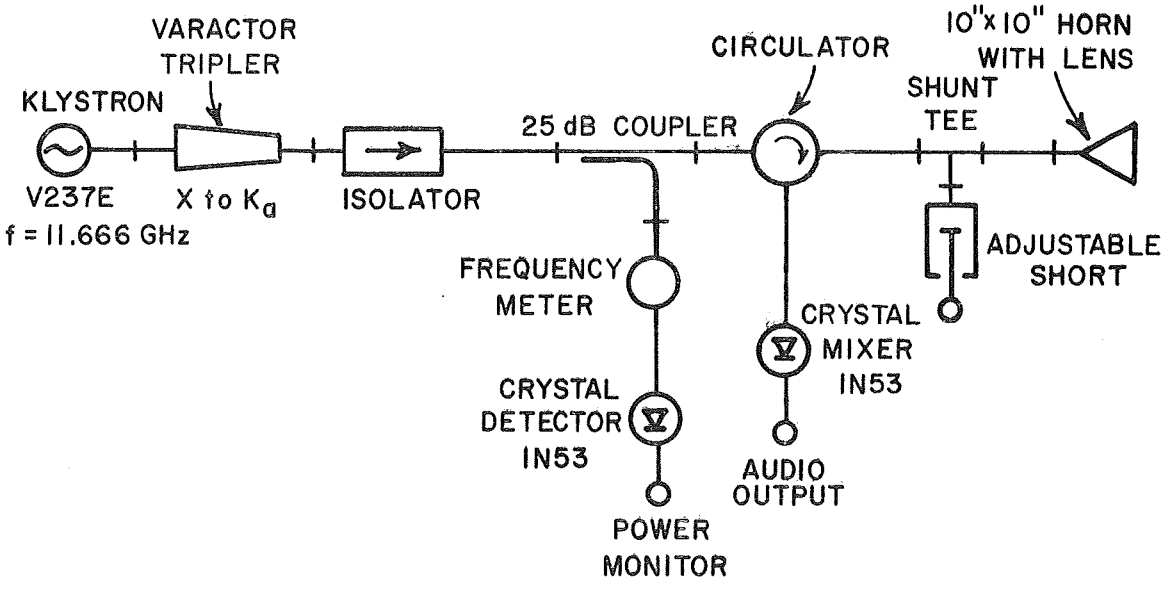

Fig. 9. K_a-band radar microwave circuit (λ=8.66 mm).

TABLE I
MICROWAVE RADAR SYSTEM SPECIFICATIONS

Frequency Wavelength	Half-Power Beamwidth (at 20')	Spot Size (sq. ft.)	Power Source	Transmitted Power (mw)	L. O. Power at Mixer (mw)
1.797 GHz 16.6 cm	12.0°	13.72	Trak Oscil-lator	398	1.5
10.0 GHz 3.0 cm	5.2°	2.59	V-249H	75	0.28-direct 0.22-cross
15.0 GHz 2.0 cm	3.76°	1.505	VA-92	97	1.0
35.0 GHz 8.66 mm	2.00°	0.382	V237E	29	0.28

The measured antenna half-power beamwidths are 12^{o} at 1.8 GHz, 5.2^{o} at 10 GHz, 3.8^{o} at 15 GHz, and 2.0^{o} at 35 GHz.

Note on Selection of L.O. Power Level

The l.o. power level must be large enough to ensure linear mixing with the largest terrain return signal likely to be encountered. The power density incident upon the area A (see Fig. 4) is

$$(5) \qquad I_o = P_o G_t/(4\pi R^2) \qquad (\text{watts}/m^2),$$

where P_o is the power radiated by the transmitting antenna, and G_t is the antenna gain. The power density scattered by the surface in the backscattering direction is

$$(6) \qquad I_s = I_o \sigma^o (\theta_i) A/(4\pi R^2) \qquad (\text{watts}/m^2),$$

where σ^o is the normalized scattering cross section. The scattered power which is received by the antenna is

$$(7) \qquad P_r = I_s \, A_{em} \qquad \text{(watts)},$$

where A_{em} is maximum effective aperture of the antenna. The ratio of the return power to the radiated power becomes

$$(8) \qquad \frac{P_r}{P_o} = \frac{G_t \, A_{em} \, \sigma^o}{(4\pi R^2)^2} \; A,$$

$$= \frac{G_t \, A_{em} \, \sigma^o}{(4\pi R^2)^2} \; \frac{\pi (R \, \theta_{HP}/2)^2}{\cos\theta_i},$$

where $\tan\left(\frac{\theta_{HP}}{2}\right) \simeq \frac{\theta_{HP}}{2}$ for narrow-beamwidth antennas. Using the fact that $G_t = 4\pi \, A_{em}/\lambda^2$, Eq. (8) becomes

$$(9) \qquad \frac{P_r}{P_o} = \frac{A^2_{em} \sigma^o (\theta_{HP})^2}{16\lambda^2 R^2 \cos\theta_i} \; .$$

For an order of magnitude calculation, the following approximations are used: the maximum effective aperture of the antenna is taken to be $A_{em} \approx 0.6 \, A_p$, where A_p is the physical area of the antenna aperture and $\cos\theta_i$ is assumed to be approximately unity. With these assumptions

$$(10) \qquad \frac{P_r}{Po} \approx \frac{0.36\sigma^o}{16} \left(\frac{A_p \theta_{HP}}{\lambda R} \right)^2 \; .$$

Because it is not intended to operate the radars near normal incidence where extremely large values of σ^o can occur over smooth surfaces, a value of $\sigma^o = 1$ has been selected as the maximum expected return. Also, linear mixing will be insured if $P_{L.O.} > 10P_r$. Thus, the l.o. power level has been chosen to be larger than that given by the following criterion:

$$(11) \qquad \frac{P_{L.O.}}{P_o} \simeq 0.225 \left(\frac{A_p \theta_{HP}}{\lambda R} \right)^2 .$$

2. Electronics

The r.f. power at S-band (1.797 GHz) is provided by a Trak oscillator, which obtains its beam voltage from a Lambda 28M Regulated Power Supply. The X-, K_u-, and K_a-band systems obtain the necessary klystron voltages from Hewlett Packard 716B Klystron Power Supplies. The K_a-band r.f. source is a varactor tripler driven by an 11.666 Ghz Klystron.

Two independent audio signal processing channels are provided. The audio voltage amplification is accomplished with Tektronix Type 122 Low-Level Preamplifiers. The normal preamplifier operating settings use a voltage gain of 100, and a bandwidth from 8 Hz to 250 Hz at X-, K_u-, and K_a-bands, and 0.8 to 250 Hz at S-band.

The Integrator and Power Monitor Module allows printout of the integrated audio signals, or the klystron power levels. The latter is also continuously monitored on a panel meter. The integrator circuit (see Fig. 10), which uses a Nexus Type CLA-3 Operational Amplifier, has

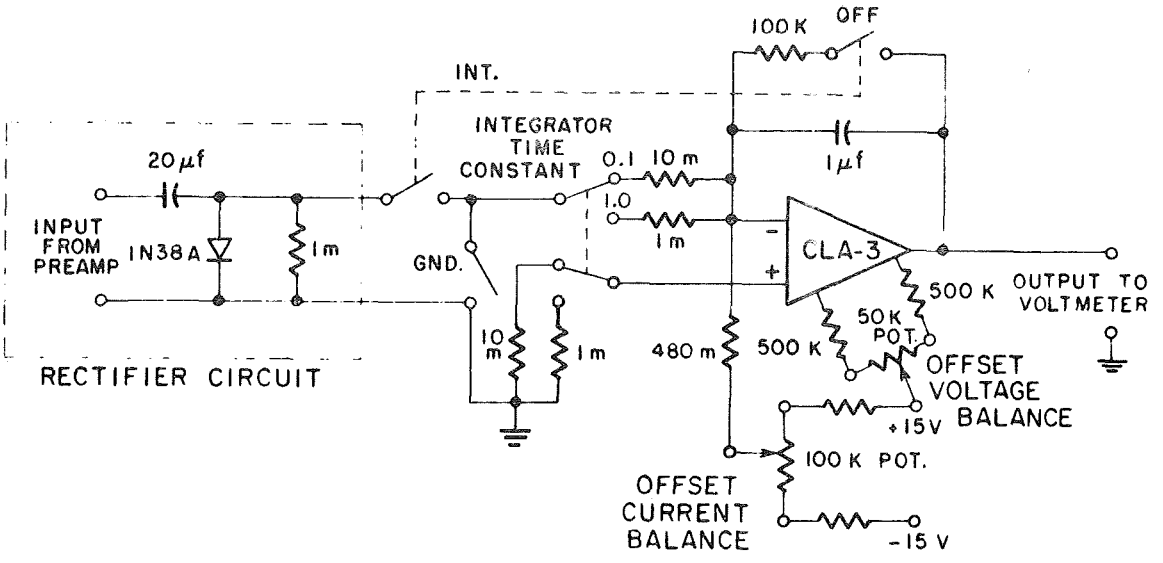

Fig. 10. Integrator-rectifier circuit.

time constants of 0.1 or 1.0 in order to utilize the full range of the integrators over the time available for each run. The amplifier features an output range of ± 10 volts with low input offset current and high stability. The rectifier portion of the integrator circuit has been calibrated for sinusoidal input voltages from 10 millivolts to 100 volts. A calibration curve of the integrator output (in seconds/volt) as a function of audio peak-to-peak input volts is shown in Fig. 11.

The integrator outputs are sampled once per second and displayed on two HP 405CR Digital Voltmeters, and the output of these is also printed on paper tape. A HP 570A Digital Clock provides the time reference and an external sampling rate command. The voltmeters provide a d.c. recording output and the print command for the HP 560A Digital Recorder.

The analog strip-chart recorder monitors the instantaneous audio

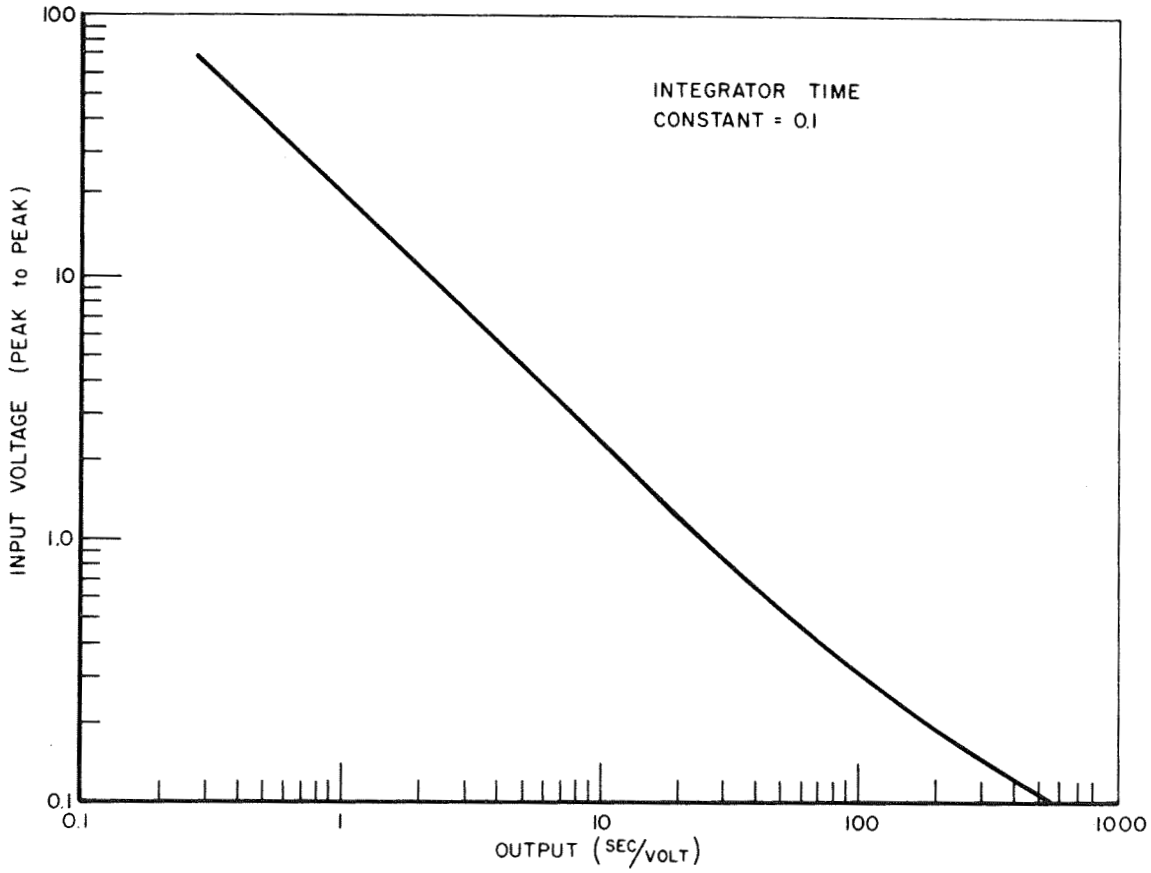

Fig. 11. Rectifier calibration curve.

terrain return signal. The analog recorder is useful for detecting anomalies in the measured terrain and for calibration alignment (see Section II-B on calibration procedure).

3. Mechanical Details

The radar boxes are secured at the end of a 40-foot movable boom which is mounted on the truck (see Fig. 1). The incidence angle is set from within the van between 0^{o} and 90^{o} using a selsyn-controlled angle indicator; however, measurements are usually made from 20^{o} to 70^{o}. A height indication dial gives the height of the boom for each operating angle so that the slant range to the terrain is always 20 feet. The microwave enclosures are manually rotated to change the operating polarization.

B. Calibration and Standards

The radar systems are calibrated on an absolute basis by comparing the return from the terrain with the return from a spherical metal target of known absolute radar cross section. To obtain the relation between the power levels in the two measurements, assume that the radar antenna has a one-way power pattern of the form $f(\psi)$ (see Fig. 12). Then the power density incident on the terrain is

$$(12) \qquad S_i = P_o G_t f(\psi)/(4\pi R^2),$$

where G_t is the maximum gain of the transmitting antenna, and R is the distance from the antenna to a point on the terrain. The power density

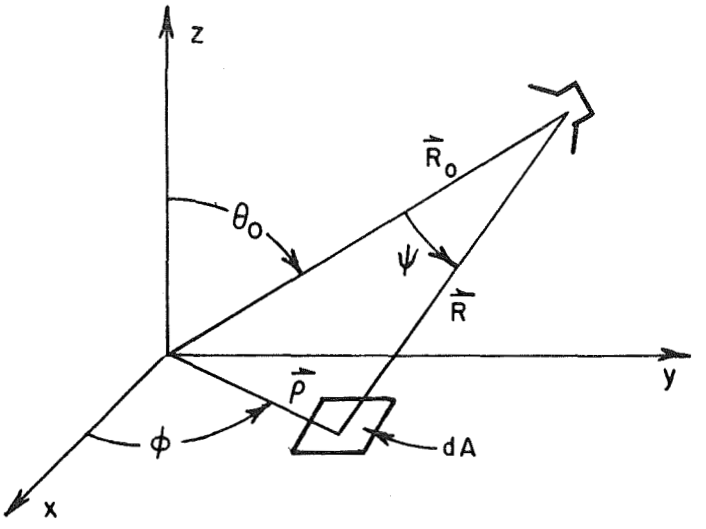

Fig. 12. Terrain backscattering geometry.

incident on the receiving antenna due to scattering by the element of area dA is given by,

$$(13) \qquad dS_r = S_i \sigma^o \, dA/(4\pi R^2).$$

The received power is then $dP_{rec} = S_r \, A_{em} \, f(\psi)$, where A_{em} is the maximum collecting aperture of the receiving antenna. Consequently, the total received power from the terrain is

$$(14) \qquad P_{rec} = \frac{P_o G_t A_{em}}{(4\pi R_o)^2} \int f^2(\psi) \, \sigma^o \left(\frac{R_o}{R}\right)^4 \frac{dA}{R_o^2} \quad ,$$

where R_o is the distance from the antenna to the center of the illuminated area. Under the same circumstances, the power returned from the standard target, placed a distance R_o from the antenna, is

$$(15) \qquad P_{st} = \frac{P_o G_t A_{em}}{(4\pi R_o^2)^2} \sigma_T \quad ,$$

where σ_T is the cross section of the standard target. Using the assumption that σ^o does not vary appreciably over the range of angles which the illuminated area subtends, σ^o may be removed from under the integral in Eq. (14,; then

$$(16) \qquad \sigma^o = \frac{P_{rec}}{P_{st}} \cdot \frac{\sigma_T}{R_o^2} \left[\int f^2(\psi) \left(\frac{R_o}{R}\right)^4 \frac{dA}{R_o^2} \right]^{-1} .$$

The factor $I = \left[\int f^2(\psi) \left(\frac{R_o}{R}\right)^4 \frac{dA}{R_o^2} \right]^{-1}$ has been evaluated by Barrick[11] for a Gaussian antenna pattern using a digital computer.

In order to see how the integral depends on the parameters describing the antenna pattern, assume that $f(\psi) = e^{-B\psi^2/2}$. Using an approximation appropriate for narrow beamwidths ($\rho/R_o << 1$); Peake[12] has demonstrated that the integral in Eq. (16) becomes

$$(17) \qquad I \approx \frac{B \cos\theta_o}{\pi} .$$

Thus, neglecting terms of order θ_{HP}^2 compared to the first order term of Eq. (17), we have

$$(18) \qquad \sigma^o \approx \frac{P_{rec}}{P_{st}} \frac{\sigma_T}{R_o^2} \frac{B\cos\theta_o}{\pi} .$$

This relatively simple calculation agrees with the numerical computation of Barrick to within $\pm$ 0.5 dB. It should be noted that Barrick's re-

sults are good only for the value of B which he assumed (B=1100). Thus, if I_B represents the value of the integral tabulated by Barrick, then

$$(19) \qquad \sigma^o \approx \frac{P_{rec}}{P_{st}} \quad \frac{\sigma_T}{R_o^2} \quad \frac{1}{I_B} \left(\frac{B}{1100}\right) \quad ,$$

where $e^{-B\psi^2/2}$ is the one-way power pattern of an actual antenna, with ψ in radians. Equation (19) represents the equation used for normalization in the radar backscattering computer program of Appendix III.

As noted at the beginning of this section, absolute calibration of the radar systems is provided by measuring the return from a spherical metal target of known cross section. To insure that the system remains stable, the transmitted signal power level is monitored before and after each set of terrain return measurements. To obtain the required doppler shift in the received signal, a counter balanced target shaker (see Fig. 13) was fabricated to replace the motion of the truck. The resultant doppler frequency, which is nearly a pure sinusoid for $r << \ell$, is given by

$$(20) \qquad f_d = \frac{2r\, w_m}{\lambda} \sin w_m t \quad \left[1 - \frac{r}{\ell} \frac{\cos w_m t}{\{1 - (\frac{r}{\ell} \sin w_m t)^2\}^{1/2}}\right] \quad ,$$

where w_m = speed of motor shaft in rad/sec,

r = offset radius of rotating arm,

ℓ = length of rotating arm,

$\lambda = f_o/c$ = wavelength of transmitted signal.

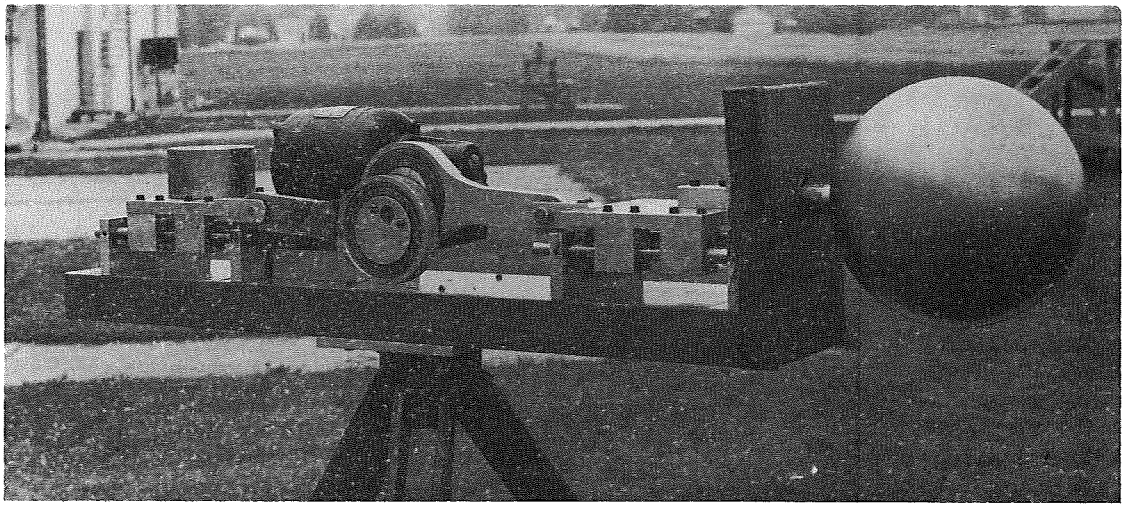

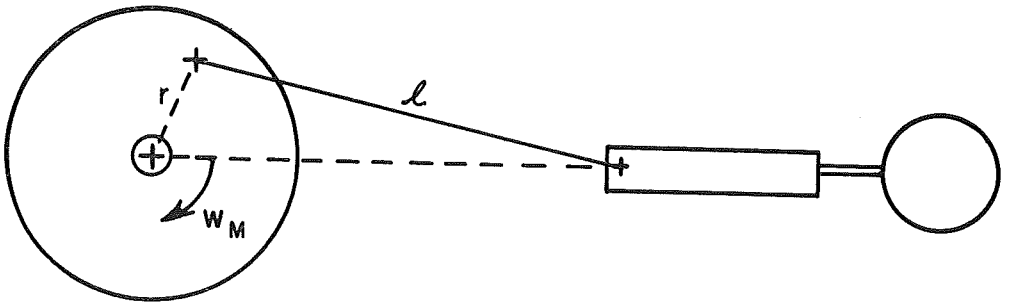

Fig. 13. Picture and geometry of the counter balanced target shaker.

The return signal from the oscillating sphere can be written as

$$(21) \qquad V_r = K\sqrt{\sigma_T}\cos 2\pi(f_o+f_d)t,$$

where K = system constant,

σ_T = cross section of the standard target,

f_o = frequency of the transmitter.

The crystal mixer output voltage is then

$$(22) \qquad V_{mix} = \frac{K\sqrt{\sigma_T}}{2}\left[\cos 2\pi f_d t + \cos 2\pi (2f_o+f_d)t\right] .$$

The audio signal from the bandpass amplifiers becomes

$$(23) \qquad V_d = \frac{K\sqrt{\sigma_T}}{2}\cos 2\pi f_d t ,$$

$$\approx \frac{K\sqrt{\sigma_T}}{2}\cos\left[(w_d \sin w_m t)\, t\right] \qquad (r << \ell),$$

where $w_d = 4\pi v_m f_o/c$,

$T = 1/w_d \sin w_m t$,

$v_m = rw_m$ = tangential velocity of the point where the rotating arm is attached to the cam.

The strip-chart recorder is required in standard calibrations to insure that the target sphere is properly bore-sighted with respect to the radar antenna (see Fig. 14). An expanded portion of the waveform, shown in Fig. 15, is seen to be approximately sinusoidal with

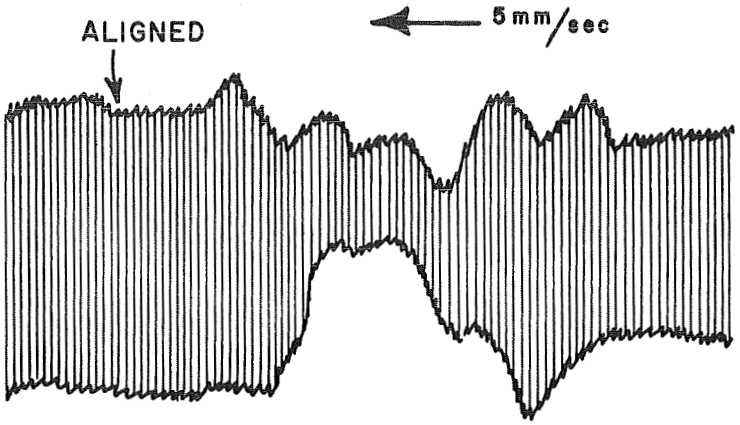

Fig. 14. Audio waveform during standard target alignment procedure of the S-band radar.

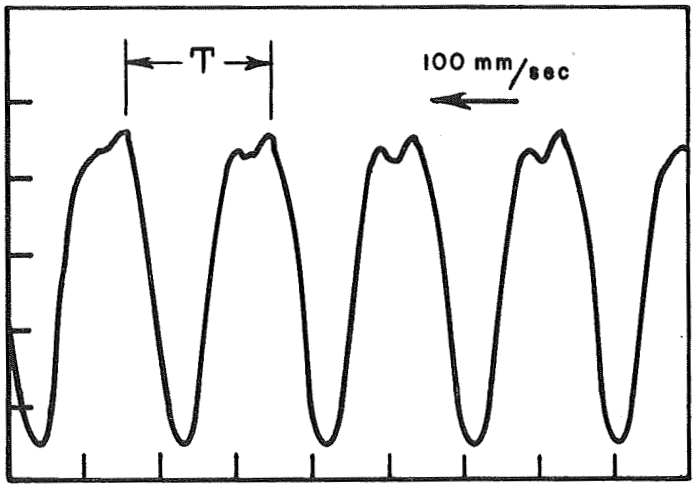

Fig. 15. Expanded portion of audio waveform shown in Fig. 14.

period, T, given by Eq. (23).

The cross-polarized channel of the X-band system is calibrated by rotating a unidirectionally conducting screen (actually an array of dipoles)[13,14] as a target (see Fig. 16). The rotation of the target modulates the reflected signal amplitude and the sidebands provide the required frequency shift for system operation. The return signals for the direct and cross-polarized channels (denoted by $V_r^{\parallel}$ and $V_r^{\perp}$, respectively) are

$$(24) \qquad V_r^{\parallel} = K\,(\sqrt{\sigma_m}\cos\theta)\cos\theta\cos 2\pi f_o t,$$

$$V_r^{\perp} = K\,(\sqrt{\sigma_m}\cos\theta)\sin\theta\cos 2\pi f_o t,$$

where K = system constant (assumed here to be the same for both channels),

σ_m = maximum scattering cross section of the dipole array,

f_o = frequency of the transmitter,

θ = angle between the incident electric field and the dipole array orientation (see Fig. 16).

The mixer outputs for the two channels are then

$$(25) \qquad V_{mix}^{\parallel} = K\sqrt{\sigma_m}\cos^2\theta\cos^2 2\pi f_o t,$$

$$V_{mix}^{\perp} = K\sqrt{\sigma_m}\cos\theta\sin\theta\cos^2 2\pi f_o t,$$

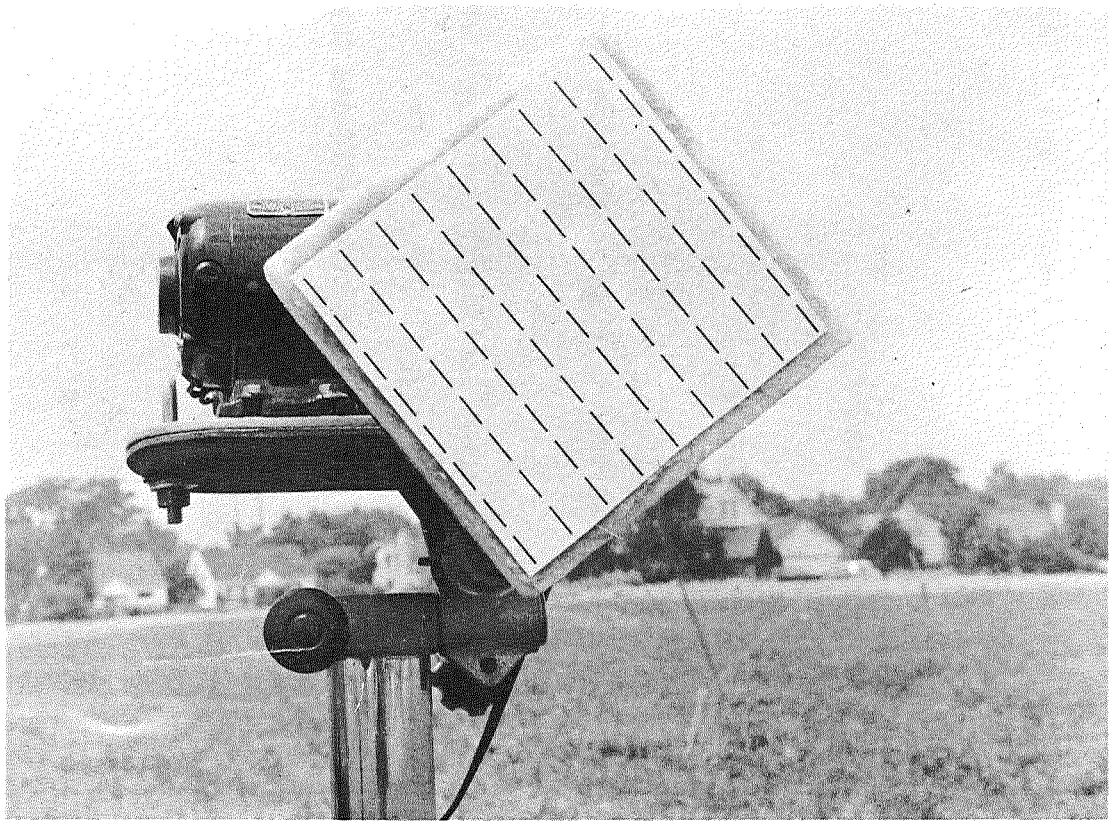

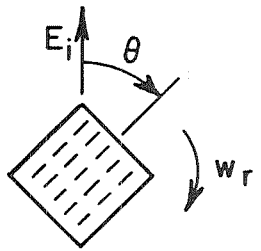

Fig. 16. Picture and geometry of X-band cross-polarized calibration target.

where $\theta = w_r t$ and w_r is the angular frequency of rotation of the target, so that the audio bandpass amplifier output voltages are (see Fig. 17)

$$(26) \qquad V_d^{\parallel} = \frac{K\sqrt{\sigma_m}}{4} \cos 2w_r t,$$

$$V_d^{\perp} = \frac{K\sqrt{\sigma_m}}{4} \sin 2w_r t \ .$$

With the assumption of equal sensitivity, K, for the two channels, the detected voltages should be equal in magnitude, at twice the frequency of the rotating target, and displaced in phase by 90^{o}. This is clearly shown by the chart recording in Fig. 17. The absolute

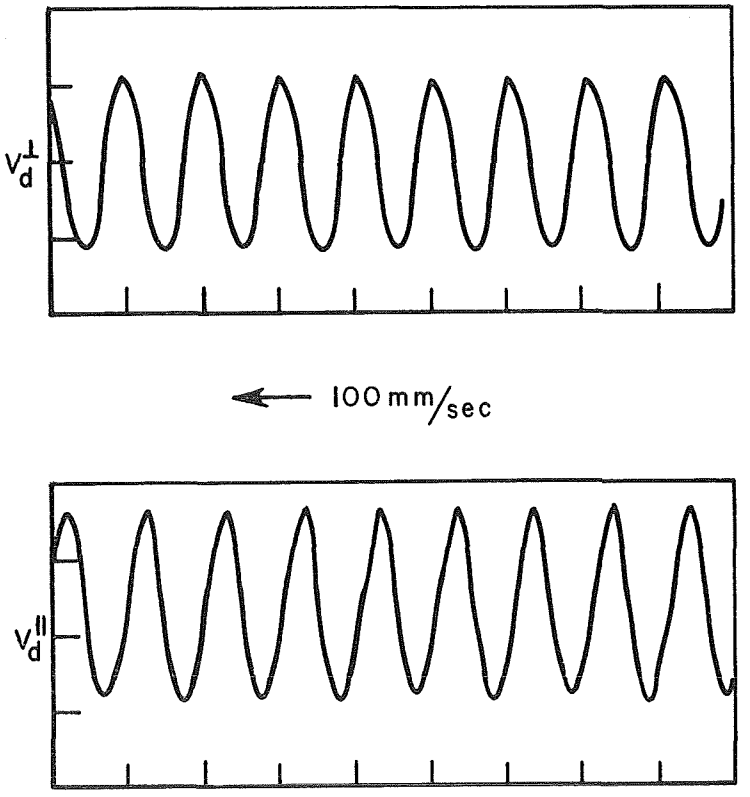

Fig. 17. The direct and cross-polarized audio signals from the X-band cross-polarized calibration standard.

calibration of the cross-polarized channel is determined relative to the previously calibrated direct channel by comparing the audio signals given by Eq. (26); the channel constants are normally unequal since they involve such parameters as amplifier gain factors and mixer l.o. levels.

The linearity of each radar system has been measured using metal spheres and corner reflectors of known echo area at the operating distance of 20 feet. The measured points are plotted in Fig. 18; the straight lines indicate the expected proportionality between received power and target cross section for each frequency.

C. Reduction of Radar Data

The reduction of the radar data entails transformation of the integrated audio signal powers from the terrain and from the standard target to a normalized radar backscattering cross section per unit area, $\sigma^o(\theta)$, using the relationship (see Section II-B for details)

$$(27) \qquad \sigma^o(\theta) = \frac{P_{rec}(\theta)}{P_{st}} \quad \frac{\sigma_T}{R_o^2} \frac{1}{I_B(\theta)} \quad \left(\frac{B}{1100}\right)$$

where P_{rec} = received power from terrain,

P_{st} = received power from standard target,

σ_T = radar cross section of standard target,

R_o = distance from antenna to target,

B = constant in exponent of one-way antenna power pattern,

I_B = value of integral tabulated by Barrick.

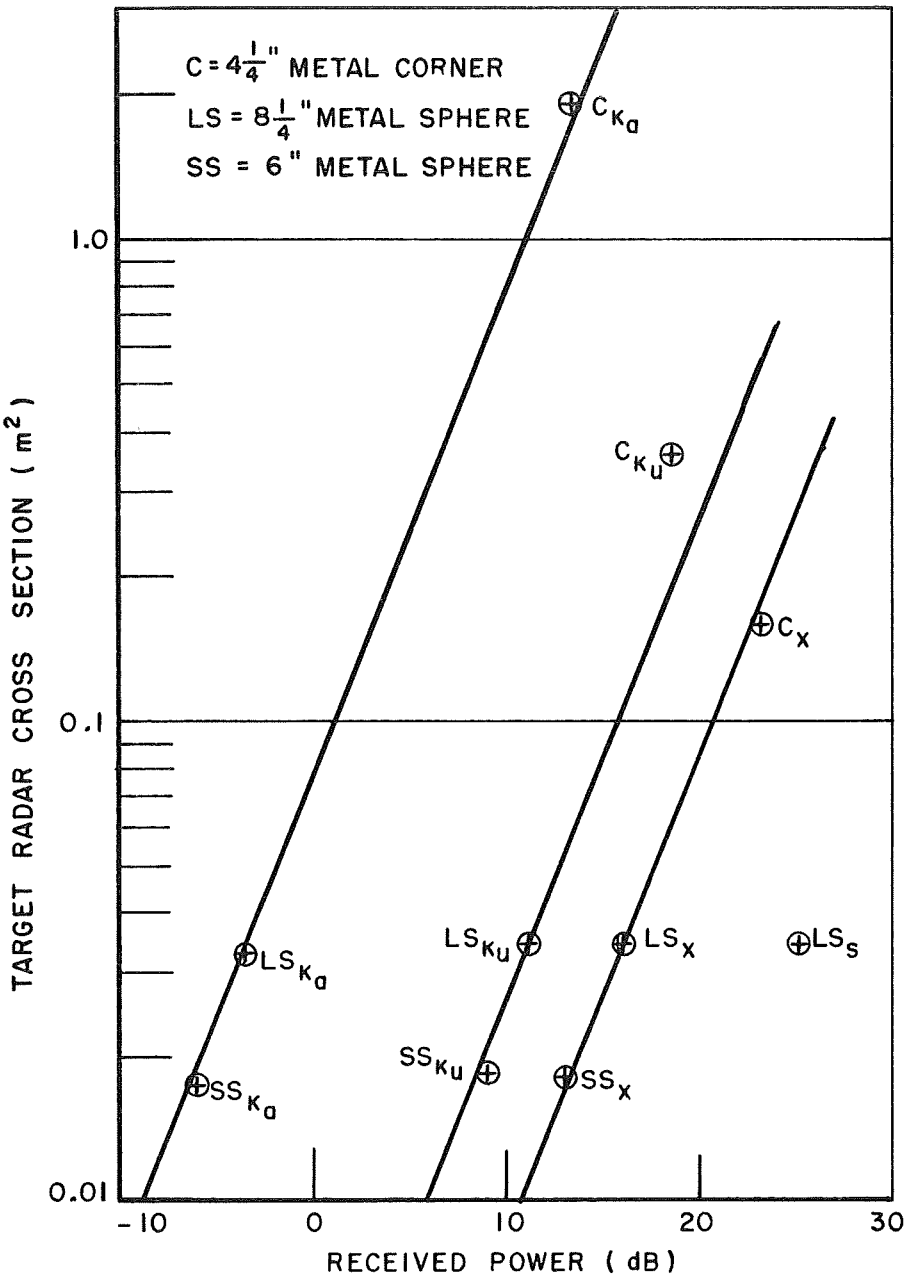

Fig. 18. Radar system linearity curves.

To perform the above computation, a high-speed digital computer is used (computer program presented in Appendix III). The computer input is derived from two sources - the digital recorder output and the radar data sheet, shown in Fig. 20. The digital recorder output format (see Fig. 19) contains the data run numbers, the time reference (one sample per second), and the sampled integrated signal voltages from the two audio channels. The radar data sheet, shown in Fig. 20, provides the necessary reference data (terrain location and identification, date, frequencies, polarizations, angles of incidence, and integrator time constants) for formulating the computer input. The computer input format, which incorporates the terrain backscattering data with a standard target calibration level for each frequency and type of terrain, is shown in Fig. 21. The "group number" is introduced into the input format to provide a convenient cross-reference between the computer input and output data; the data is presently catalogued as follows: groups 1-99 correspond to data obtained in 1965, groups 100-199 in 1966, and so forth. The "time" is the interval in seconds between two selected samples on the digital paper tape print-out. The "volt" column represents the difference between the integrator output at the end and the beginning of the selected interval. The average power P_{rec} in Eq. (27), is then a function of the ratio ("seconds/volt") of these two quantities for the terrain; the power P_{st} from the standard sphere, is the corresponding ratio from the calibration run.

The computer output is a paper print-out of both $\sigma^{o}(\theta)$ and $\gamma(\theta)$, and optional punched cards for the plotting of $\gamma(\theta)$ vsθ. The print-out

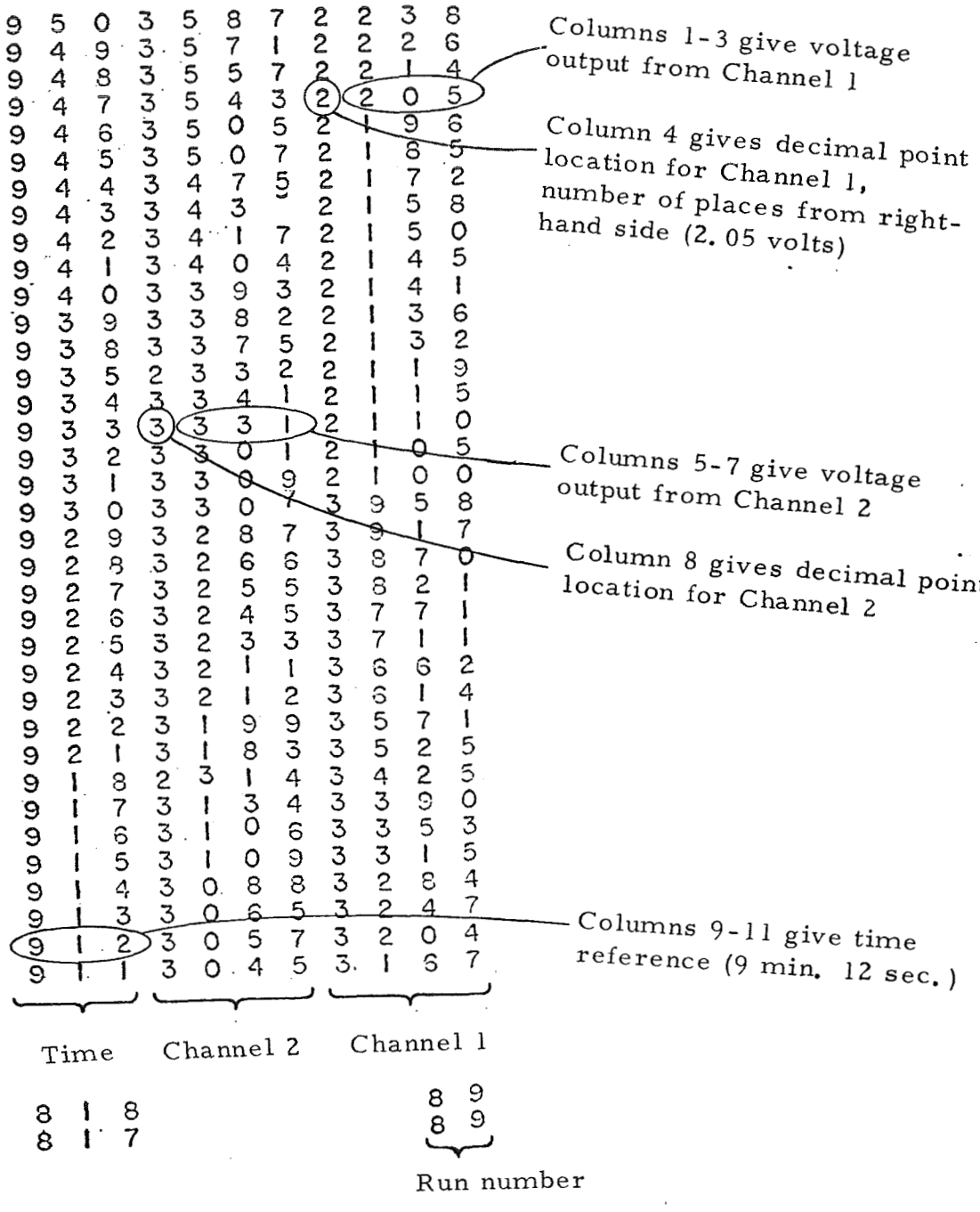

Fig. 19. Digital recorder output format.

RADAR DATA

TERRAIN

LOCATION

DATA

DRY BULB

WET BULB

WIND

TARGET KEY

S = 8" SPHERE

D = DIPOLE ARRAY

ANGLES MEASURED FROM NORMAL

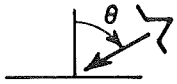

TIME	RUN	CHANNEL 1 FREQ.	POL.	ANGLE OR TARGET	T.C.	B.W.	PWR.	CHANNEL 2 FREQ.	POL.	ANGLE OR TARGET	T.C.	B.W.	PWR.

Fig. 20. Radar data reference sheet.

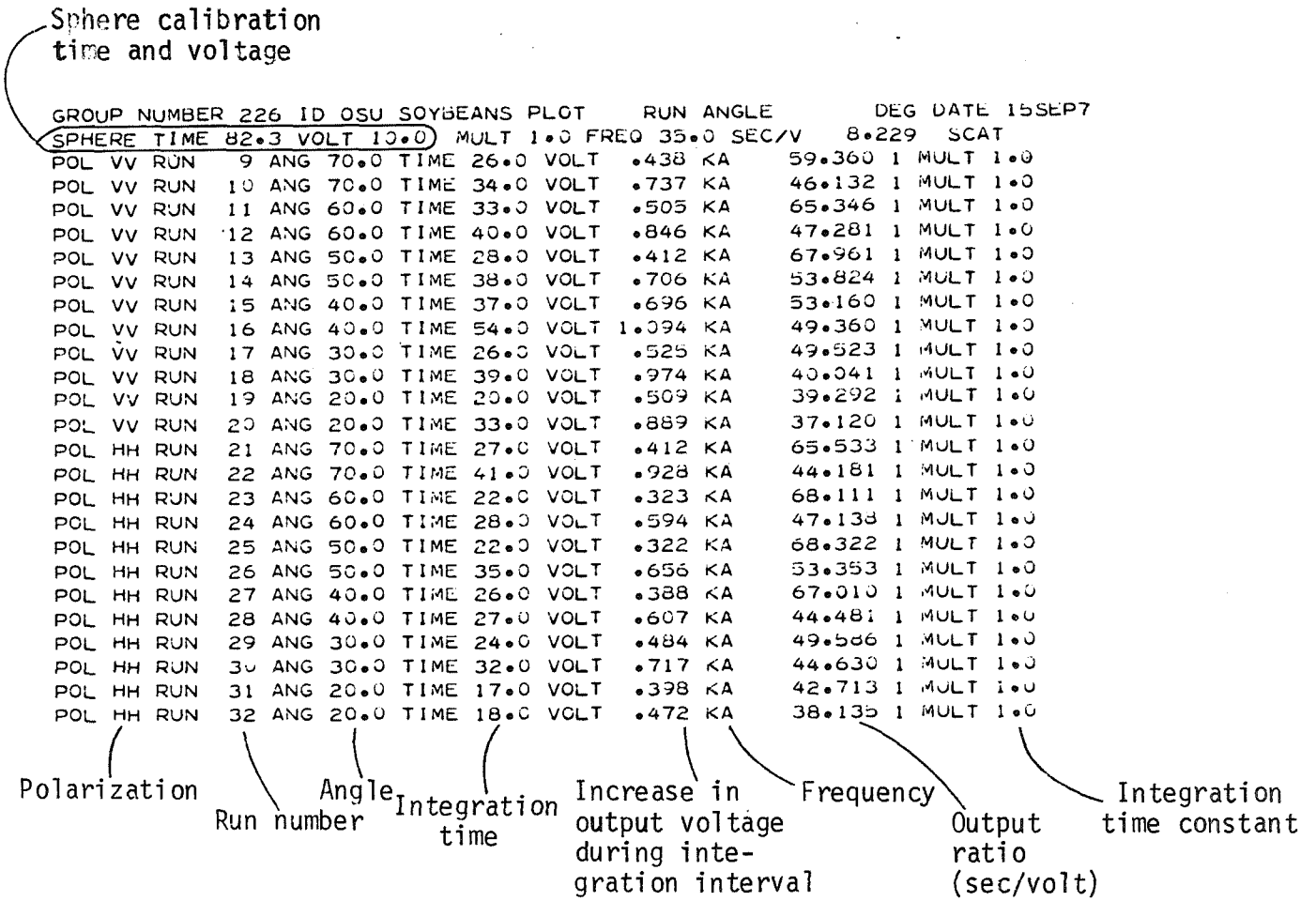

Fig. 21. Radar data computer input format.

format (see Fig. 22) also provides for terrain identification, date, frequency, and a standard target calibration level (in dB). The sample plot format for $\gamma(\theta)$, shown in Fig. 23, utilizes an overlay for axes labeling and the polarization key, in order to save plotting time. The polarization subscripts for γ are indicated in the key accompaning each plot.

MEASURED BACKSCATTERING CROSS SECTION PER UNIT AREA VS. INCIDENCE ANGLE FROM NORMAL

DATA GROUP NUMBER = 226 TERRAIN OSU SOYBEANS FREQUENCY = 35.000 GIGAHERTZ
DATE 15SEP7

NO PLOTS REQUESTED

INTEGRATION TIME FROM REFERENCE SPHERE = 82.3[illegible] SECONDS VOLTAGE 10.[illegible] VOLTS MULTIPLIER 1.[illegible]
TIME/VOLT 8.23[illegible] INPUT [illegible].35642 IN DB -8.9607[illegible] FREQUENCY 35.0

VERTICAL POLARIZATION

RUN NUMBER	BACKSCATTERING ANGLE	ABSOLUTE CROSS SECTION	CROSS SECTION IN DECIBELS	GAMMA IN DECIBELS
9	70.[illegible]	[illegible].03105351	-15.[illegible]79	-10.419
10	70.[illegible]	[illegible].04257841	-13.708	-9.049
11	60.[illegible]	[illegible].04072120	-13.932	-10.891
12	60.[illegible]	[illegible].06166154	-12.142	-9.132
13	50.[illegible]	[illegible].05077342	-12.944	-11.024
14	50.[illegible]	[illegible].06798943	-11.676	-9.756
15	40.[illegible]	[illegible].08324740	-10.796	-9.639
16	40.[illegible]	[illegible].09134929	-10.393	-9.235
17	30.[illegible]	[illegible].10356973	-9.848	-9.223
18	30.[illegible]	[illegible].13514591	-8.692	-8.067
19	20.[illegible]	[illegible].15077082	-8.217	-7.947
20	20.[illegible]	[illegible].16189808	-7.908	-7.637

HORIZONTAL POLARIZATION

RUN NUMBER	BACKSCATTERING ANGLE	ABSOLUTE CROSS SECTION	CROSS SECTION IN DECIBELS	GAMMA IN DECIBELS
21	70.[illegible]	[illegible].02743567	-15.617	-10.957
22	70.[illegible]	[illegible].04494656	-13.473	-8.814
23	60.[illegible]	[illegible].03866229	-14.127	-11.117
24	60.[illegible]	[illegible].06129400	-12.126	-9.116
25	50.[illegible]	[illegible].05043701	-12.973	-11.053
26	50.[illegible]	[illegible].06874125	-11.628	-9.709
27	40.[illegible]	[illegible].06229930	-12.055	-10.898
28	40.[illegible]	[illegible].11406323	-9.427	-8.670
29	30.[illegible]	[illegible].12840510	-9.855	-9.230
30	30.[illegible]	[illegible].11797832	-9.282	-8.657
31	20.[illegible]	[illegible].13580875	-8.671	-8.401
32	20.[illegible]	[illegible].15652020	-8.054	-7.784

Fig. 22. Radar data computer print-out format.

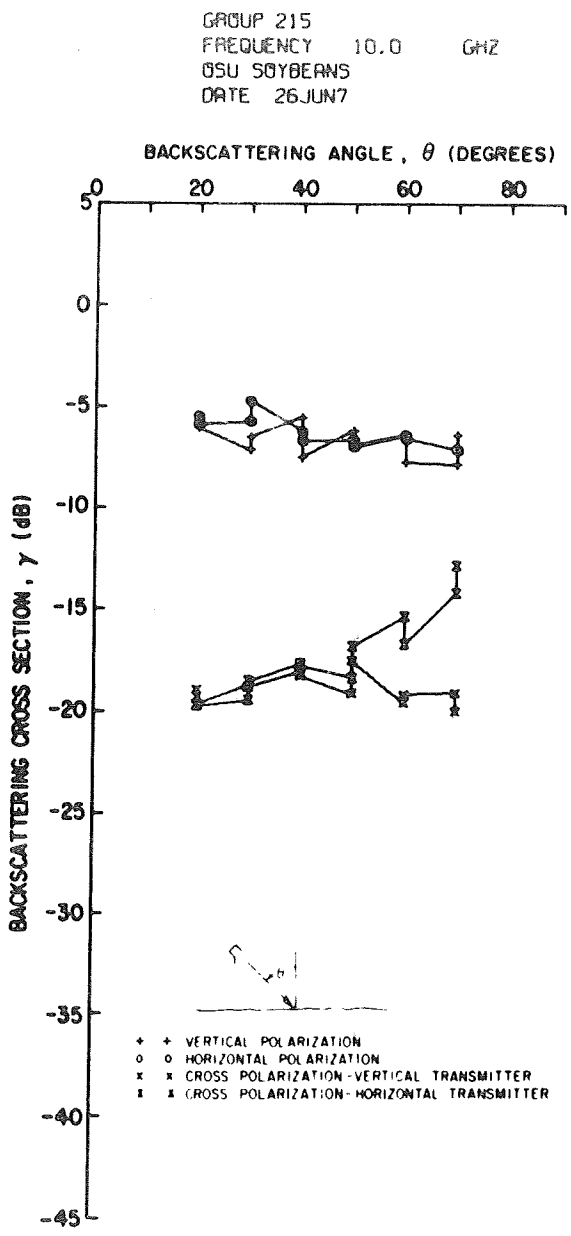

Fig. 23. Radar data computer plotting format for $\gamma(\theta)$.

CHAPTER III

RADIOMETER FACILITIES

The O.S.U. radiometer facility consists of two microwave Dicke-type radiometers (10 GHz and 35 GHz) with sensitivities of the order of two or three degrees Kelvin, designed to measure the brightness temperature of an antenna viewing the terrain. Calibration is by means of an internal oven load with an attenuator to obtain hot ($358^{o}K$) and ambient reference temperatures. The microwave portions of the radiometers are contained in boxes which can be mounted on the end of the same hydraulic boom used to support the radar systems (see Fig. 1). Any linear polarization may be obtained by rotating the box, and any look angle from zenith to nadir may be selected from inside the van.

The purpose of the radiometer measurements is to determine the brightness temperature of the terrain, $T(\theta)$, which is a weighted average of the brightness temperature incident on the antenna and the antenna power pattern,[15] given by

$$(28) \qquad T_{ant}(\theta_o) = \frac{\int_0^{2\pi}\int_0^{\pi} T(\theta)\, f(\theta',\phi')\, \sin\theta'\, d\theta'\, d\phi'}{\int_0^{2\pi}\int_0^{\pi} f(\theta',\phi')\, \sin\theta'\, d\theta'\, d\phi'} ,$$

where $T_{ant}(\theta_o)$ = brightness temperature measured by an antenna looking in the θ_o-direction,

$T(\theta)$ = the unknown brightness temperature distribution of the surface,

$f(\theta',\phi')$ = normalized antenna power pattern function,

$\sin\theta' \, d\theta' \, d\phi'$ = element of solid angle (see Fig. 24).

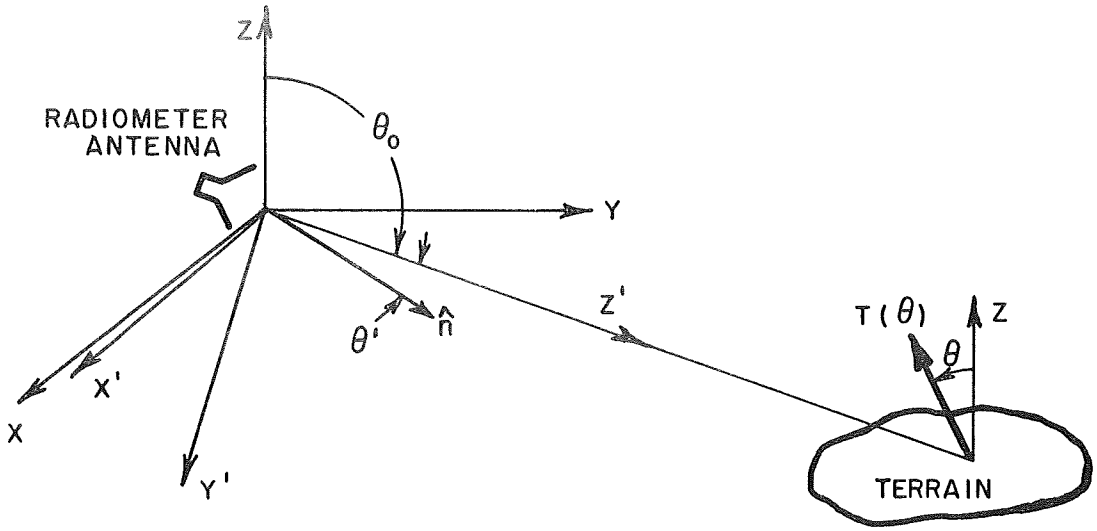

Fig. 24. Geometry of radiometer problem.

The inversion of the integral in Eq. (28) to obtain the brightness temperature, $T(\theta)$, will be discussed in Section III-C.

As alluded to previously, there is also a relation between the brightness temperature and the bistatic radar return parameter of the terrain. The total brightness temperature of natural terrain surfaces is the sum of emission and sky reflected radiation. It has been shown by Peake,[16] that the total brightness temperature at ground level, as seen by an antenna viewing the surface from the direction i with polarization j, is (see Fig. 25)

$$(29) \qquad T_j(i) = e_j(i)\, T_g + (4\pi)^{-1} \int \left[\gamma_{jj}(i,s) + \gamma_{jk}(i,s)\right] T_{sky}(s)\, d\Omega_s,$$

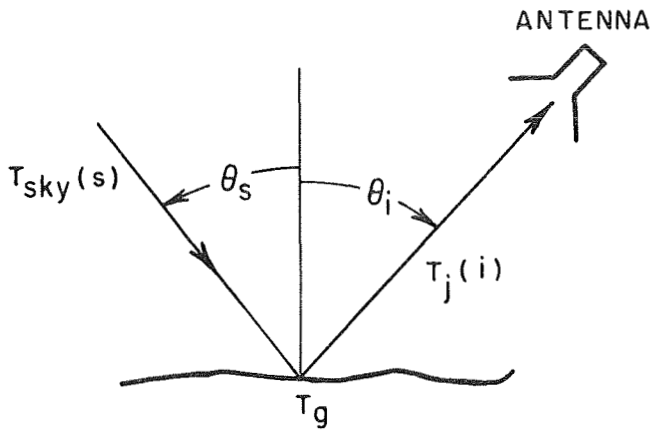

Fig. 25. Geometry for the brightness temperature scattering parameter relationship.

where $e_j(i)$ = emission coefficient of the surface,

T_g = physical temperature of the surface,

γ = bistatic radar return parameters per unit "projected" area,

T_{sky} = downward sky radiation temperature.

In many cases, particularly for a clear sky and $\theta_s < 80^o$, the downward sky radiation temperature can be expressed as

$$(30) \qquad T_{sky}(\theta_s) = (1.12\, T_{air} - 50)\left[1-(1-\alpha_o)^{\sec\theta_s}\right] \quad ,$$

where T_{air} = temperature of the atmosphere measured at ground level (in ^oK),

α_o = total zenith attenuation,

θ_s = angle measured from zenith (in radians).

This formula, with Eq. (29), can be used to estimate T_{ant} in the inversion integral if the coefficients γ_{jk} are known. Also, Eq. (30) is often useful in estimating the zenith sky temperature as a secondary calibration check.

To compute the total brightness temperature given by Eq. (29), the emission coefficient of the surface must be known. From Kirchhoff's radiation law, the emission coefficient is equal to the absorption coefficient,[8] i.e.,

$$e_j(i) = a_j(i), \tag{31}$$

where the absorption coefficient is defined as that fraction of the power incident on a surface of area $A\cos\theta_i$ from direction $\theta_i \phi_i$ with polarization state j(see Fig. 4), that is not rescattered. With this definition, the emission coefficient can be expressed in terms of the bistatic scattering cross section as

$$e_j(i) = 1 - \frac{\int I_s R^2 \, d\Omega s}{I_o A \cos\theta_i} \tag{32}$$

$$= 1 - (4\pi)^{-1} \int \left[\gamma_{jj}(i,s) + \gamma_{jk}(i,s)\right] \, d\Omega_s \ ,$$

where the integration is over the upper hemisphere. Thus, from Eqs. (29) and (32), the brightness temperature of the surface is determined by certain weighted averages of the bistatic coefficients γ_{jk}. The radar return, on the other hand, is just $\gamma_{jk}(i,i)$. This connection between the two sensor responses (i.e., the brightness temperature and

the backscattering) is the reason for desiring to measure both sensor outputs simultaneously (see Ref. 7).

A. Systems

The functional components of the radiometer system, shown in Fig. 26, consist of a microwave ferrite switch which alternately switches the input to the mixer between the antenna, at temperature T_{ant}, and the ambient reference load, at temperature T_L. A balanced microwave mixer is used to down-convert the modulated signal to an IF frequency, where it is then amplified by the preamp and IF amplifier, whose pass-band determine the r.f. system bandwidth. The envelope of the amplified IF signal is recovered by a crystal detector and passed through a narrowband, 1000Hz amplifier. Final detection is accomplished by a synchronous demodulator, whose inputs are a 1000 Hz reference signal and the signal from the selective amplifier. The demodulator output is a D.C. voltage proportional to the difference between the temperatures of the ambient reference load and the antenna. The manually-operated waveguide switch is used for switching from the antenna to the oven load during calibrations (see discussion in Section III-B).

The criterion used in evaluating the performance of a radiometer is its minimum detectable temperature sensitivity,[17] ΔT, which can be expressed as

$$\Delta T \simeq \kappa\,(F-1)T_o/\sqrt{B\tau} \quad , \tag{33}$$

if the system gain fluctuations are neglected;

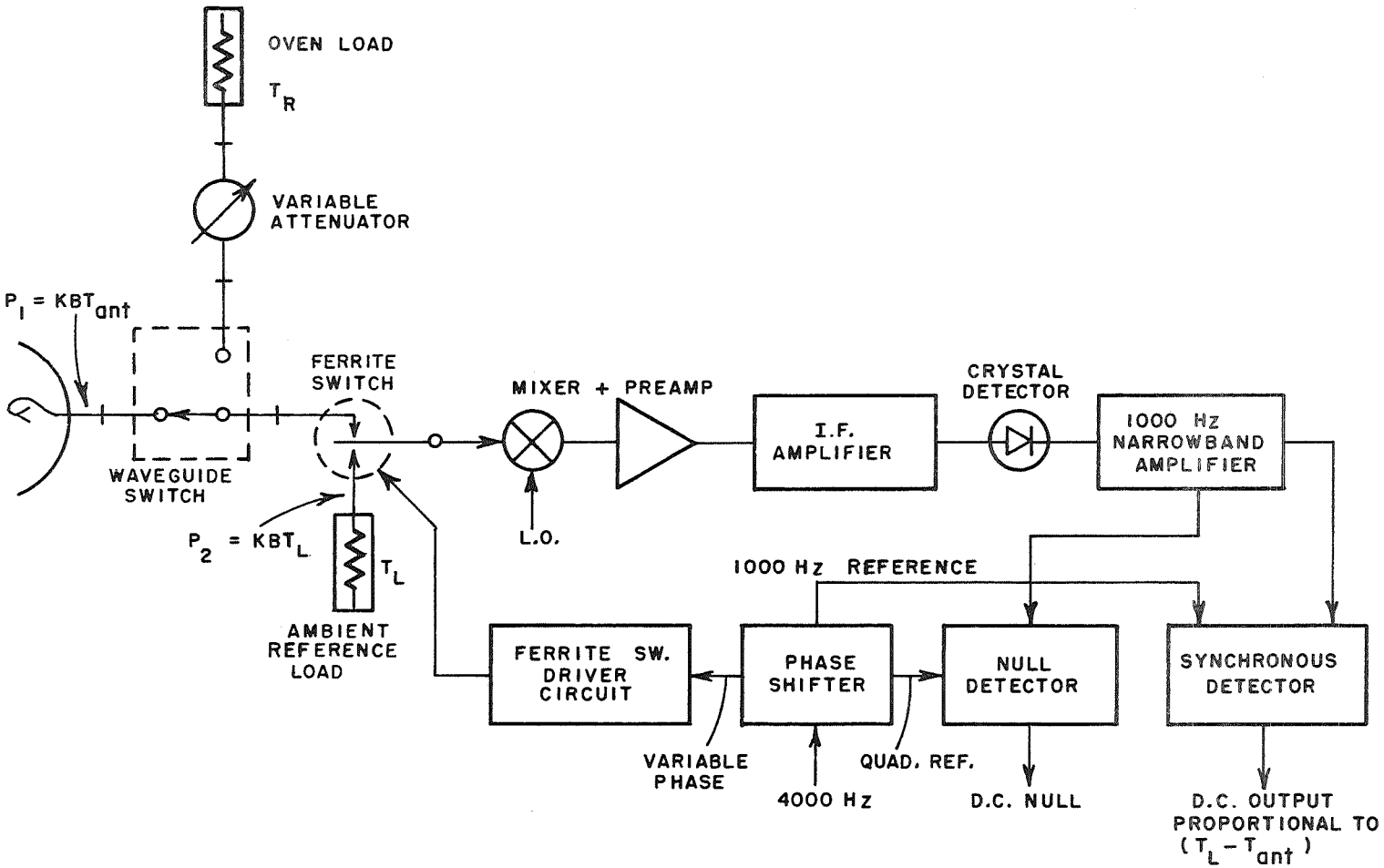

Fig. 26. Block diagram of a typical radiometer system.

where κ = a system constant depending on modulation, detection factors, and other system parameters,

$T_o = 290^oK$,

F = system noise figure,

B = predetection bandwidth,

τ = postdetection integration time.

A summary of the system parameters and performance characteristics for the two radiometers is presented in Section III-A-3.

1. Microwave

The microwave systems are mounted in thermally insulated enclosures, as shown in Fig. 27. The X-band and K_a-band microwave circuits are shown in Figs. 28 and 29, respectively. The l.o. power necessary for operation of the mixer (see Fig. 26), is provided by reflex klystrons. The mixer-preamplifiers have IF bandwidths of 2 MHz to 250 MHz, and RF to IF power gains of 20 dB. The antenna patterns are presented in Appendix II.

2. Electronics

The IF amplifier (see Fig. 26) has a maximum power gain of 45 dB with a nominal bandwidth of 10 MHz to 250 MHz, and a measured "double side band" bandwidth of 350 MHz. This bandwidth controls the predetection bandwidth, B, of the system. For postdetection gain, a 1000Hz narrow band amplifier, shown in Fig. 30, is used; the maximum voltage amplification is 10^5 and the bandwidth is 78 Hz. However, the postdetection

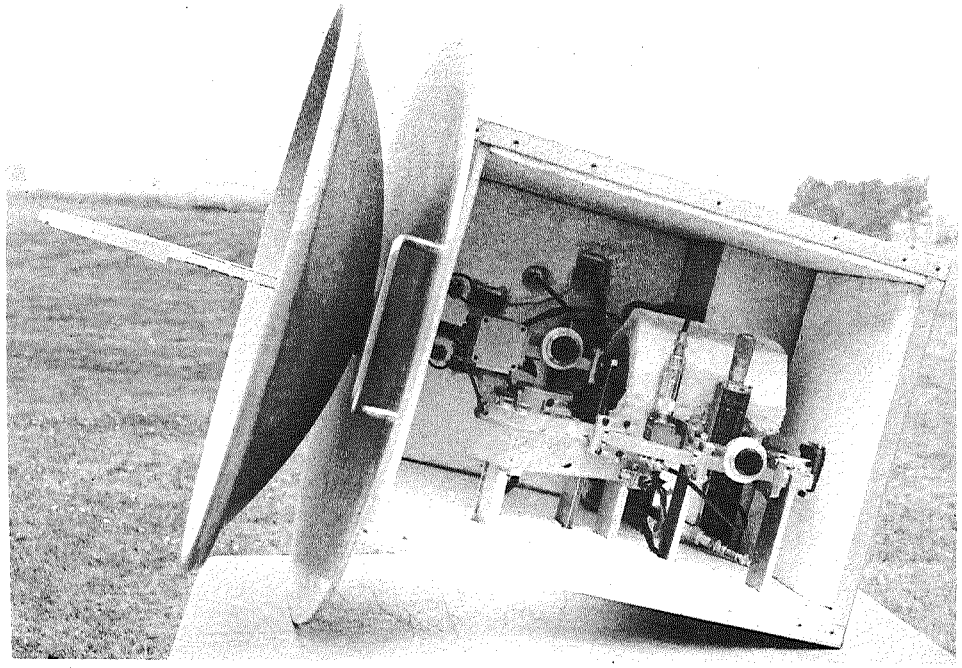

Fig. 27. Picture of X-band radiometer enclosure.

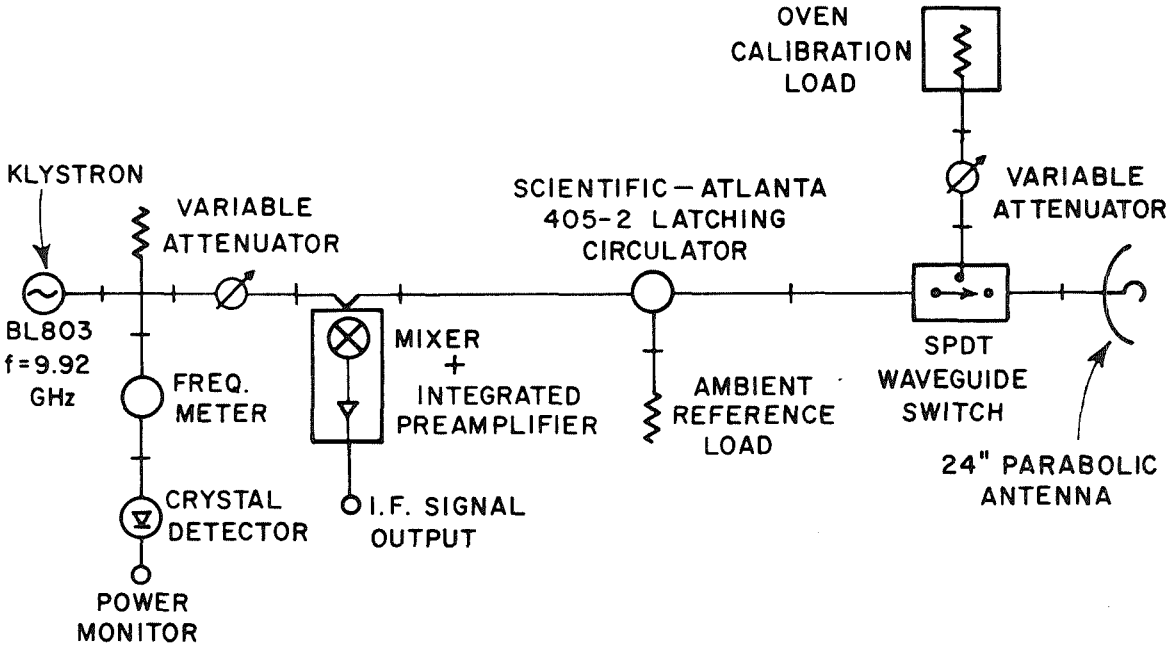

Fig. 28. X-band radiometer microwave circuit (f=10 GHz).

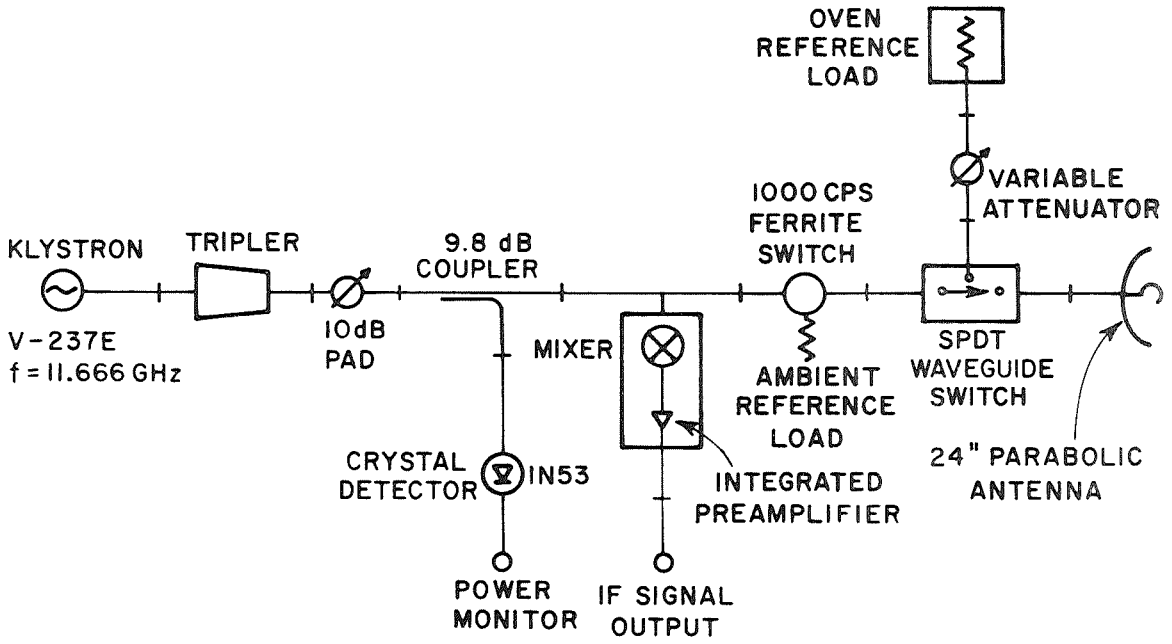

Fig. 29. K_a-band radiometer microwave circuit (f=35 GHz).

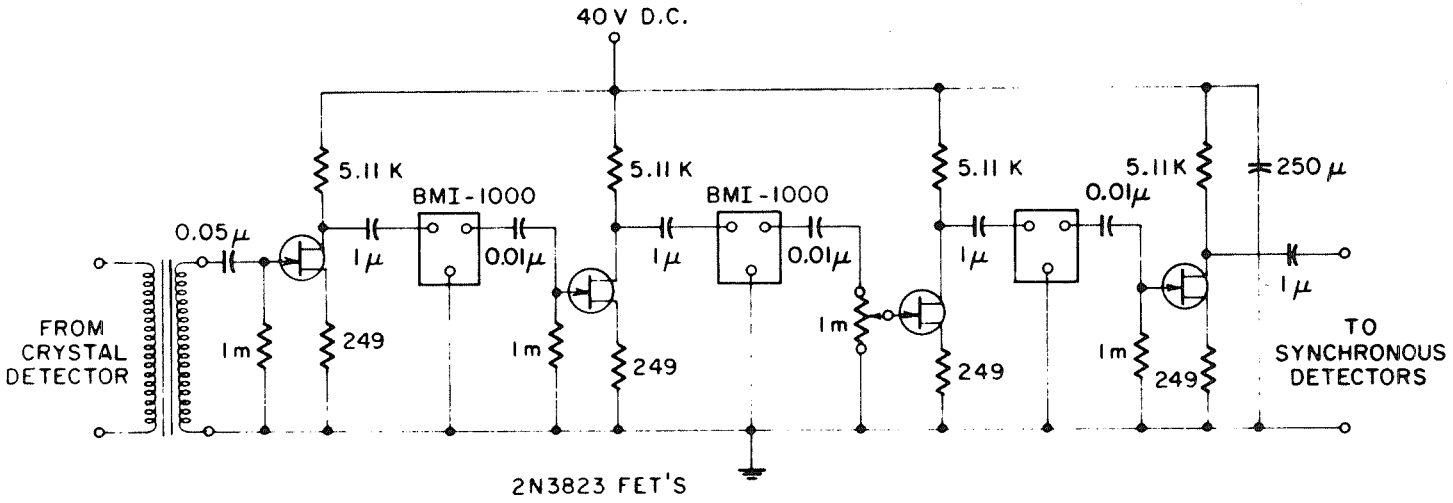

Fig. 30. 1000Hz narrow-band amplifier.

bandwidth in Eq. (33) is determined by the final integrator time constant, which is the order of 5 seconds.

For synchronous detection of the modulated signal, a 4000 Hz fork is used to provide the master timing reference. Using a frequency-division technique (see Fig. 31), 1000 Hz in-phase and quadrature reference signals are derived from this master oscillator; the quadrature reference has a 90^{o} phase differential relative to the in-phase reference. Both this 90^{o} phase differential and the 180^{o} on-off times of the in-phase and quadrature waveforms are independent of the 4000Hz waveform symmetry, as shown in timing waveforms 3 and 4 in Fig. 31. The synchronous and quadrature detectors, shown in Fig. 32, are identical circuits, both of which receive a 1000 Hz input signal from the narrowband amplifier. The quadrature detector is desirable because it produces a null output when the in-phase detector output is maximized; thus, it provides a convenient check of the phase adjustment for synchronous detection. The detector outputs are observed on a HP 412A DC Voltmeter.

In addition to the reference signals for synchronous detection, the 1000Hz phase-shifting network is used to obtain variable-phase driving waveforms for the ferrite switch driver circuits, shown in Fig. 33. The switch drivers were designed to produce desirable r.f. waveforms; i.e., equal duty cycles and maximum on-off amplitude ratio (see Fig. 34) of the r.f. signal.

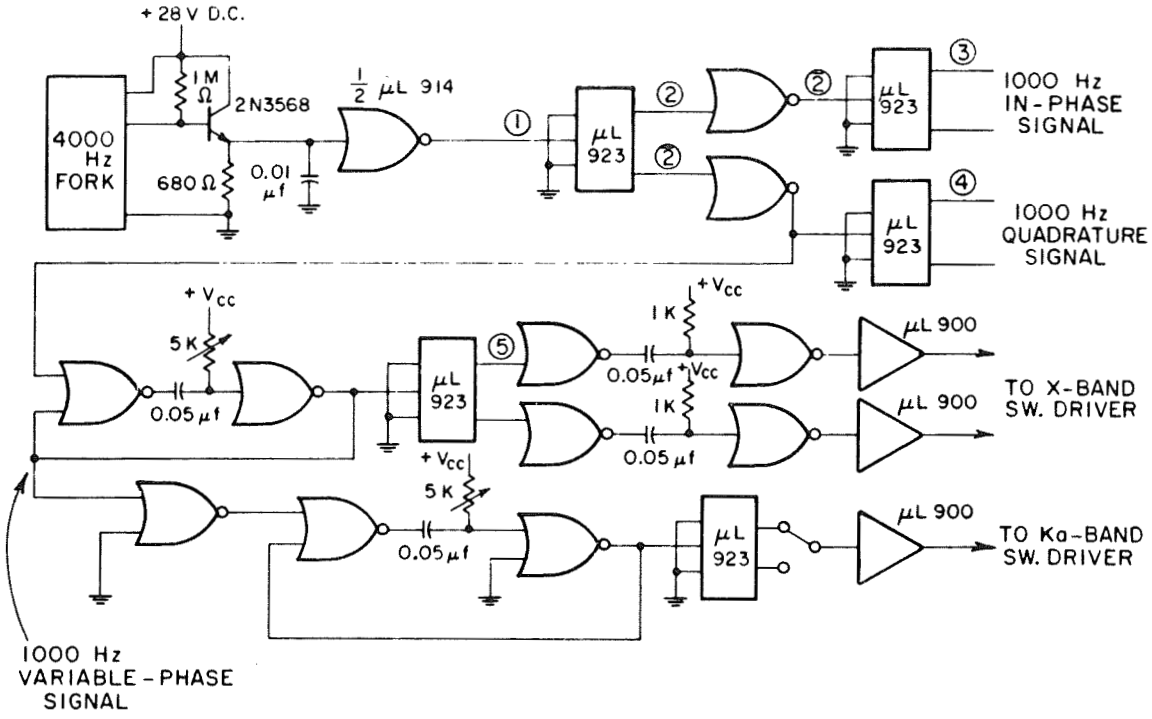

(a) BLOCK DIAGRAM

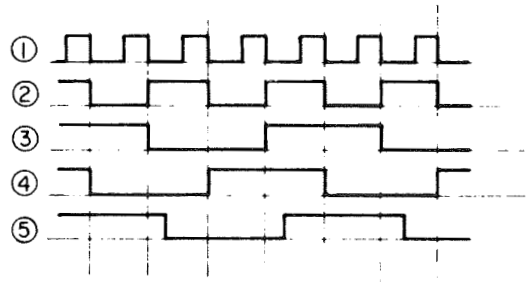

(b) TYPICAL TIMING WAVEFORMS

Fig. 31. 1000Hz phase-shifting network using RTL-circuitry.

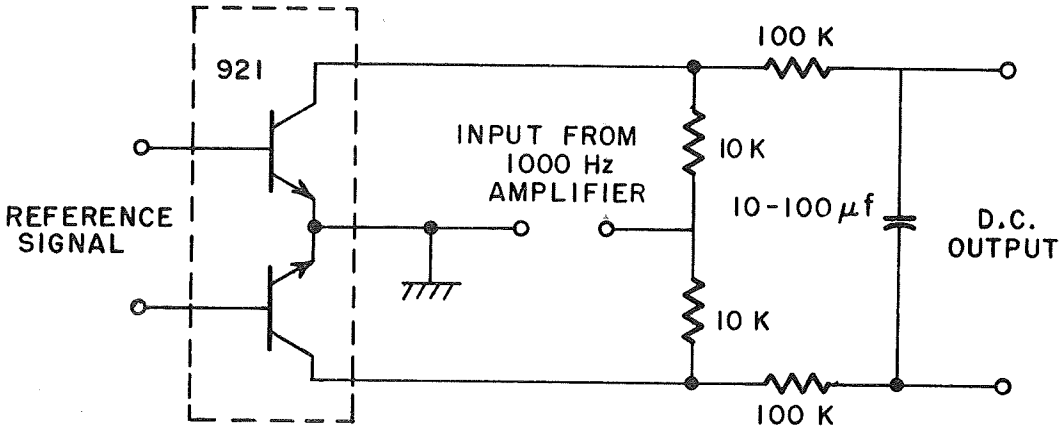

Fig. 32. Synchronous detector circuit.

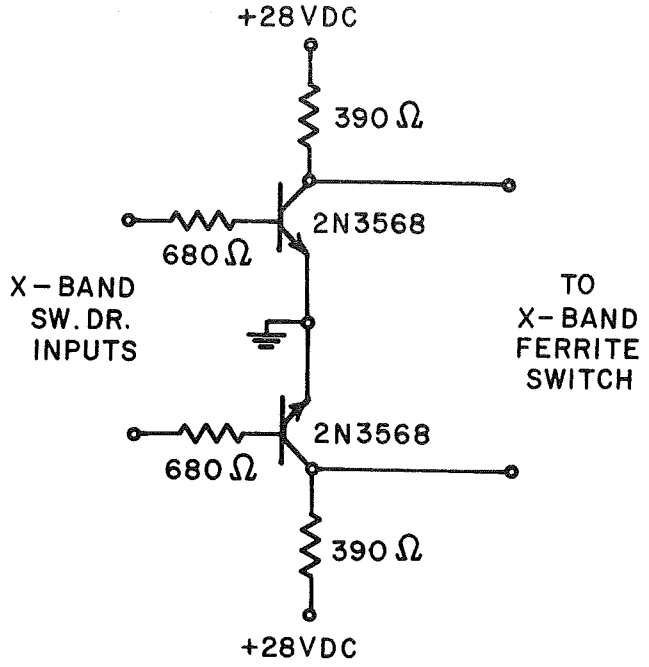

(a) X-BAND RADIOMETER

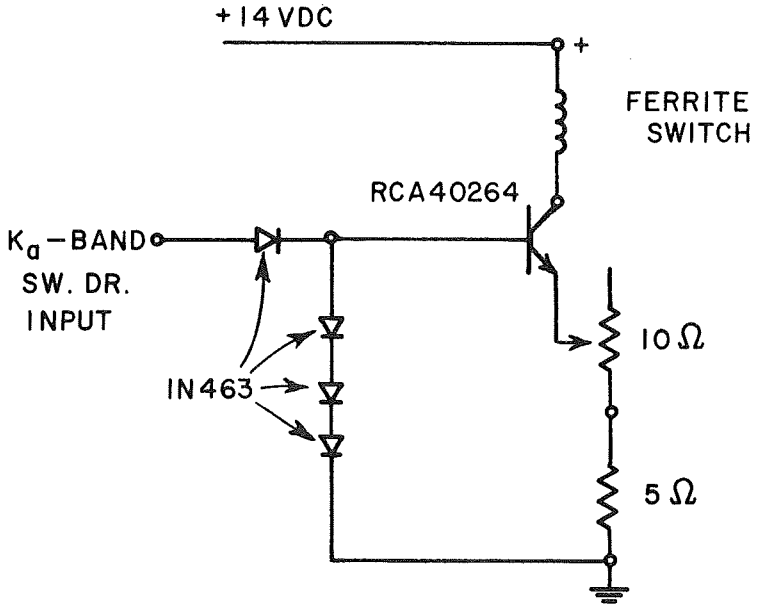

(b) K_a-BAND RADIOMETER

Fig. 33. Ferrite switch driver circuits.

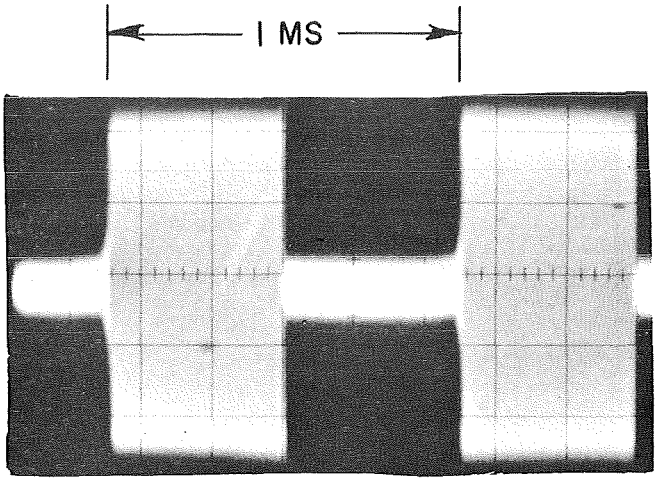

Fig. 34. The envelope of the amplified IF signal of the X-band radiometer.

3. Summary of Performance

The performance characteristics of the two radiometer systems are summarized in Table II.[15]

TABLE II

SUMMARY OF RADIOMETER CHARACTERISTICS

		X-Band	K_a-Band
1.	Calculated ΔT with τ =5 seconds time and radiometer constant κ =5	0.48°K	0.96°K
2.	Measured ΔT with same integration time, τ	0.75°K	1.5°K
3.	Measured noise bandwidth (DSB), B	350 MHz	350 MHz
4.	Measured noise figure, F	12.5±0.5 dB	15.7±0.5 dB
5.	Antenna beamwidth	3.5°	1.5°
6.	Antenna VSWR (maximum over frequency range used)	1.09	1.10

TABLE II (continued)

		X-Band	K_a-Band
7.	Oven load and attenuator VSWR		
	0 dB attenuation	1.06	1.06
	20 dB attenuation	1.04	1.05
8.	Reference load VSWR	1.02	1.05
9.	Predetection power gain	60 dB	60 dB
10.	Postdetection voltage amplification	10^5	10^5

B. Calibrations

1. System parameters

The method used for calibration is to refer all temperatures to the input of the mixer, which requires accurate measurement of all waveguide losses from the antenna to the mixer and of the attenuation characteristics of the ferrite switch (Fig. 35). The purpose of the oven load is to provide a known, internal temperature which replaces the unknown antenna temperature during calibrations. When the manually-operated waveguide switch connects receiver and antenna (port 3), the radiation temperature at the mixer is

$$(34) \qquad T_{mix}^{ant} = \alpha_8 [\alpha_6 [\alpha_5 [\alpha_3 [\alpha_1 T_{ant} + (1-\alpha_1)T_1] + (1-\alpha_3) T_3] + (1-\alpha_5)T_5] + (1-\alpha_6)T_6] + (1-\alpha_8)T_8 ,$$

where α_1 = transmission coefficient from antenna feed to waveguide switch,

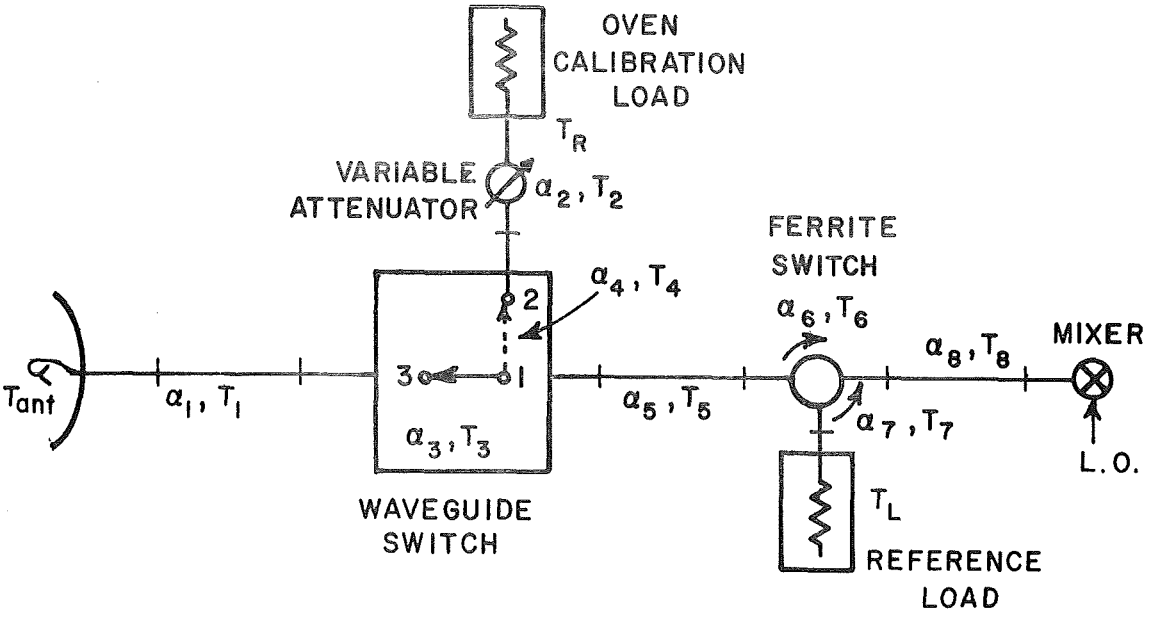

Fig. 35. System calibrations.

α_2 = transmission coefficient of variable attenuator,

α_3 = transmission coefficient from port 3 to port 1 of waveguide switch,

α_4 = transmission coefficient from port 2 to port 1 of waveguide switch,

α_5 = transmission coefficient from waveguide switch to ferrite switch,

α_6 = transmission coefficient from port 2 to port 1 of ferrite switch,

α_7 = transmission coefficient from port 3 to port 1 of ferrite switch,

α_8 = transmission coefficient from ferrite switch to mixer,

$T_1, T_2, \ldots, T_8$ = corresponding thermal waveguide temperatures,

T_{ant} = effective antenna temperature,

T_R = oven calibration load temperature (358^oK),

T_L = reference load temperature.

For calibrations, the waveguide switch connects the receiver to the oven load (port 2), and the temperature at the mixer is

$$(35) \qquad T_{mix}^{calib} = \alpha_8[\alpha_6[\alpha_5[\alpha_4[\alpha_2 T_R + (1-\alpha_2)T_2] + (1-\alpha_4)T_4] + (1-\alpha_5)T_5] + (1-\alpha_6)T_6] + (1-\alpha_8)T_8$$

where

$$\alpha_2 = \begin{cases} \alpha'_2 \text{ , transmission coefficient when attenuator setting is 20 dB (corresponding to ambient calibration),} \\ \alpha''_2 \text{ , transmission coefficient when attenuator setting is 0 dB (corresponding to oven calibration).} \end{cases}$$

Similarly, the temperature at the mixer with the reference load connected is

$$(36) \qquad T_{mix}^{ref} = \alpha_8 [\alpha_7 T_L + (1-\alpha_7) T_7] + (1-\alpha_8) T_8 .$$

Utilizing the fact that the system is linear,[15]

$$(37) \qquad V_{out} = K [T_{mix} - T_{mix}^{ref}]$$

where T_{mix} may be either T_{mix}^{ant} or T_{mix}^{calib}.

In actual operation, the oven is allowed to reach its equilibrium temperature, T_R, prior to the calibrations and remains at that value throughout. The components of the box come into equilibrium and with the exception of T_1, the waveguide temperatures will then stabilize at the same physical temperature as the reference load, T_L. Thus, $T_L=T_2,T_3,\ldots, T_8$ and the resulting output voltage equations become:

$$(38) \qquad V_o^{ant} = K\ \alpha_8\alpha_6\alpha_5\alpha_3\ [\alpha_1 T_{ant} + (1-\alpha_1)\ T_1-T_L]\ ,$$

$$(39) \qquad V_o^{calib} = K\ \alpha_8\alpha_6\alpha_5\alpha_4\alpha_2\ (T_R-T_L).$$

The unknown antenna temperature, T_{ant}, is determined by setting up the following relationships for the ambient and oven calibrations:

$$(40) \qquad V_o^{ant} - V_o^{amb} = K\ \alpha_8\alpha_6\alpha_5\{\alpha_3[\alpha_1 T_{ant}+(1-\alpha_1)T_1-T_L] - \alpha_4\alpha'_2(T_R-T_L)\}\ ,$$

$$(41) \qquad V_o^{amb} - V_o^{oven} = K\ \alpha_8\alpha_6\alpha_5\{\alpha_4(\alpha'_2- \alpha''_2)(T_R-T_L)\}\ .$$

Dividing Eq. (40) by Eq. (41), the resultant expression becomes

$$(42) \qquad \left(\frac{V_o^{ant} - V_o^{amb}}{V_o^{amb} - V_o^{oven}}\right) = \frac{\alpha_3\ [\alpha_1 T_{ant} + (1-\alpha_1)T_1-T_L] - \alpha_4\alpha'_2\ (T_R-T_L)}{\alpha_4\ (\alpha'_2-\alpha''_2)\ (T_R-T_L)}.$$

Solving for T_{ant}, we have

$$(43) \qquad T_{ant}(\theta_o) = \frac{1}{\alpha_1}\left\{T_L - (1-\alpha_1)T_1 + \frac{\alpha_4}{\alpha_3}[T_R-T_L]\left[\alpha'_2 + (\alpha'_2-\alpha''_2)\left(\frac{V_o^{ant}(\theta_o) - V_o^{amb}}{V_o^{amb}-V_o^{oven}}\right)\right]\right\}$$

for the radiation temperature of the antenna in terms of measured voltages, the known attenuation factors, and the physical temperatures of the components, (T_L, T_R, T_1).

2. Field calibration procedure

The reference temperatures used in the calibration procedure are those corresponding to V_o^{amb} and V_o^{oven}; V_o^{amb} is measured with the attenuator setting at 20 dB, and V_o^{oven} with a 0 dB setting. These measured voltages, the waveguide transmission factors, and the waveguide temperatures (monitored by thermistors) are all that are required to calculate $T_{ant}(\theta_o)$ from the measured output voltages $V_o^{ant}(\theta_o)$. Calibration is also checked by inserting a matched load at known temperature directly into the antenna feed, and by zenith sky measurements.

C. Reduction of Radiometer Data

The d.c. output voltages corresponding to the antenna and calibration temperatures are recorded on the radiometer data sheet (see Fig. 36), together with the waveguide temperatures and auxiliary ground truth measurements (for example, air and ground temperatures and wind

RADIOMETER DATA

FREQUENCY

TERRAIN

LOCATION

COMMENTS

DATE

TIME

DRY BULB

WET BULB

WIND

ANGLES MEASURED FROM NADIR 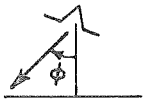

TIME								
T_{BOX}								
T_{ANT}								
T_{GROUND}								
T_{AIR}								

TIME	ANGLE OR CALIBRATION	OUTPUT VOLTAGE	POL.

TIME	ANGLE OR CALIBRATION	OUTPUT VOLTAGE	POL.

Fig. 36. Radiometer data sheet.

velocity) necessary for computing the antenna temperatures. The computer program for reducing these input data to antenna temperatures, according to Eq. (43), is given in Appendix IV.

These computed antenna temperatures and corresponding angles from zenith, the frequency,polarization, and date, are read into another computer program (presented in Appendix V) to obtain the brightness temperature by inversion of the integral equation, Eq. (28). The computer input format is shown in Fig. 37. The inversion of integrals of this type is discussed by Twomey[18]; however in view of measurement uncertainties, a simple bootstrap method of inversion is used here. The integral is initially evaluated using the measured values of $T_{ant}(\theta_o)$ as first approximations to $T(\theta)$, to compute corresponding values of "$T_{ant}(\theta)$", i.e., to compute what the antenna temperatures would be if the brightness temperatures were the same as the measured $T_{ant}(\theta_o)$. Then, to check the validity of this first estimate, these computed antenna temperatures are compared with the measured values. If the difference ΔT_1 is not sufficiently small, a new estimate of the brightness temperature $T_1(\theta)$ is obtained by subtracting ΔT_1 from $T_{ant}(\theta_o)$. This new estimate is then used to get a second set of computed antenna temperatures which are again compared with the measured values, the difference being designated ΔT_2. The iterations are terminated after three or four passes, since there is no guarantee that the procedure will converge. However, for the cases computed, all values of ΔT have reduced to within a few degrees Kelvin by termination.

The output format for the brightness temperature program is

Terrain	Location	Date	Frequency	Polarization
WHEAT	OSU FARM	3JUL68	10.0	HORIZ
	0.	14.70		WHEAT X H 3JUL68
	10.	13.60		WHEAT X H 3JUL68
	20.	12.52		WHEAT X H 3JUL68
	30.	11.44		WHEAT X H 3JUL68
	40.	14.70		WHEAT X H 3JUL68
	50.	17.96		WHEAT X H 3JUL68
	60.	21.22		WHEAT X H 3JUL68
	70.	27.73		WHEAT X H 3JUL68
	80.	30.99		WHEAT X H 3JUL68
	90.	112.43		WHEAT X H 3JUL68
	100.	229.71		WHEAT X H 3JUL68
	110.	239.48		WHEAT X H 3JUL68
	120.	249.26		WHEAT X H 3JUL68
	130.	250.88		WHEAT X H 3JUL68
	140.	254.14		WHEAT X H 3JUL68
	150.	255.77		WHEAT X H 3JUL68
	160.	259.03		WHEAT X H 3JUL68
	170.	262.29		WHEAT X H 3JUL68
	180.	263.92		WHEAT X H 3JUL68

Angle from zenith T_{ant}

Fig. 37. Brightness temperature computer input format.

shown in Fig. 38, and presents the type of terrain, location, date, the frequency, and polarization. The column listings are angles from zenith (THETA), the measured antenna temperatures (TALSO), the successive values of the difference between the measured and computed antenna temperatures (DELTA T), and the successive values of the estimated brightness temperature (TEMP). The measured antenna temperatures and computed brightness temperatures of the surface presented in Fig. 38, are plotted in Fig. 39.

Accuracy of measurements

Although the measured minimum detectable temperature is the order of $3^{o}K$, the precision of measurement is determined more by calibration uncertainties (particularly the oven temperature and waveguide losses) and by the inversion procedure (including errors in the antenna pattern

function) than by the inherent statistical fluctuations, ΔT. It is estimated, from Eq. (43), that a $1^{o}K$ uncertainty in the oven temperature will result in an error of approximately $5^{o}K$ in the zenith sky temperature. However, most terrain surfaces have antenna temperatures between $200^{o}K$ and $300^{o}K$; in this range, calibration errors will be comparable to the uncertainty in the oven temperature. Thus, it is expected that the absolute accuracy in measuring the antenna temperature is of the order of $5^{o}K$, and the relative accuracy (between measurements on a given surface at different angles or polarizations) is of the order of $3^{o}K$.

TERRAIN WHEAT

LOCATION OSU FARM DATE 3JUL68

FREQUENCY 10.0 GHZ VERT POLARIZATION

THETA	TALSO	DELTA T1	TEMP1	DELTA T2	TEMP2	DELTA T3	TEMP3
0.	14.7	-14.3	0.4	-0.4	0.0	0.5	0.5
10.	16.9	-13.8	3.0	-0.2	2.8	0.7	3.5
20.	19.0	-14.9	4.1	-0.8	3.3	0.4	3.7
30.	21.2	-17.3	3.9	-2.3	1.7	-0.2	1.5
40.	23.4	-19.2	4.2	-3.3	0.9	-0.6	0.2
50.	25.6	-20.3	5.2	-3.9	1.3	-0.8	0.5
60.	27.7	-21.4	6.3	-4.4	2.0	-0.9	1.1
70.	31.0	-23.0	8.0	-5.2	2.8	-1.2	1.6
80.	47.3	-22.6	24.7	-6.0	18.7	-1.6	17.1
90.	105.9	-10.7	95.2	-3.9	91.2	-1.5	89.7
100.	229.7	26.8	256.5	8.4	264.9	2.8	267.7
110.	242.7	23.1	265.8	5.0	270.8	1.0	271.9
120.	249.3	22.4	271.7	4.6	276.2	1.0	277.2
130.	252.5	21.5	274.0	4.0	278.0	0.8	278.8
140.	259.0	22.1	281.2	4.2	285.3	0.9	286.2
150.	259.0	19.9	278.9	3.1	282.0	0.4	282.4
160.	260.7	18.0	278.6	1.9	280.6	-0.0	280.5
170.	262.3	16.8	279.1	1.3	280.4	-0.3	280.1
180.	262.3	16.4	278.7	1.1	279.8	-0.3	279.5
Angle from zenith	T_{ant}		$T_1(\theta)$		$T_2(\theta)$		$T_3(\theta)$

Fig. 38. Brightness temperature computer output format.

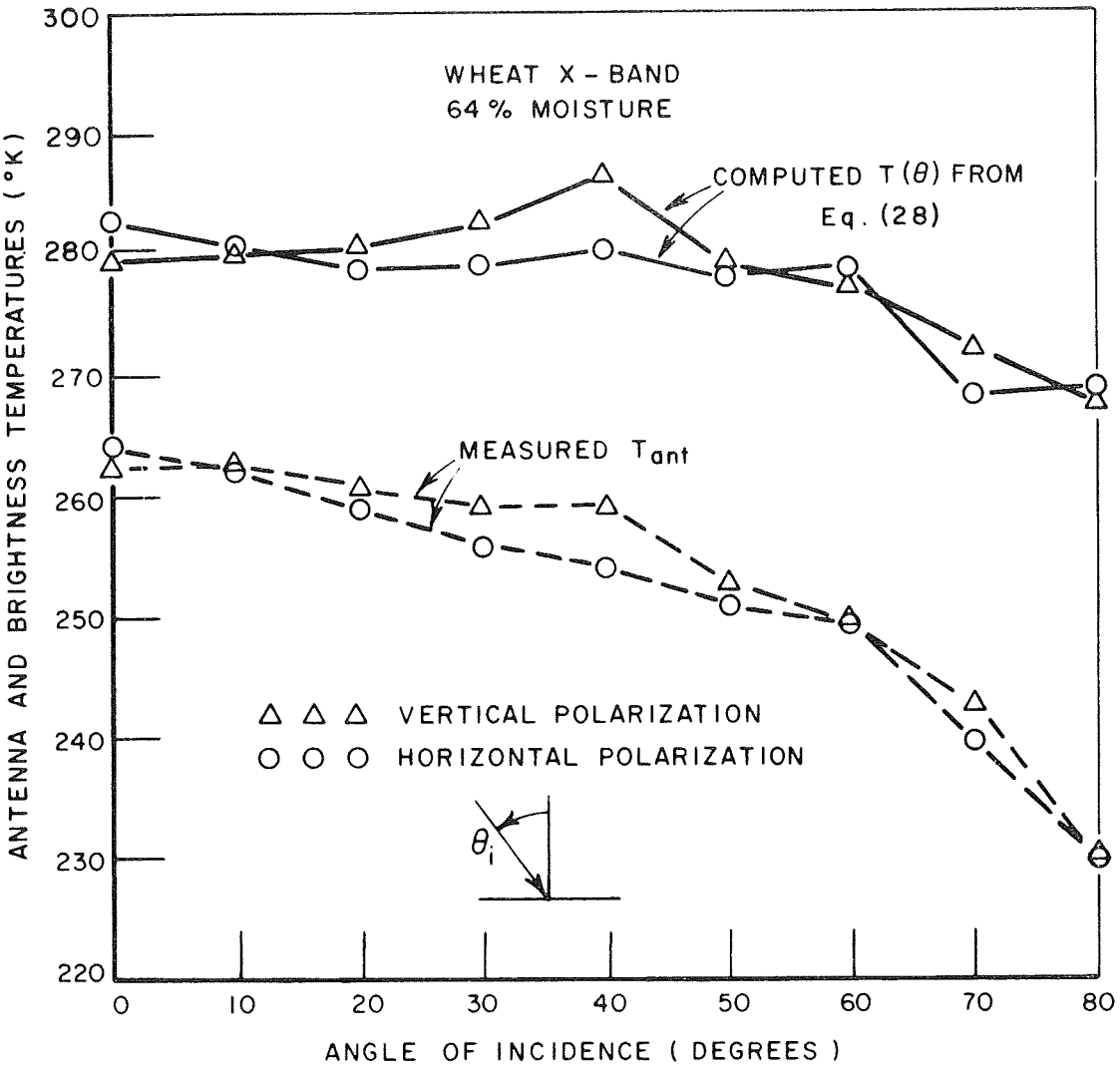

Fig. 39. Measured antenna temperatures and computed brightness temperatures of wheat at X-band (3 July 1968).

CHAPTER IV

SUMMARY AND CONCLUSIONS

This report has described the design and construction of a mobile facility for measuring the backscattering and brightness temperature of terrain at microwave frequencies, with emphasis on the operational theory, system circuitry and parameter specification, and the data reduction procedures.

Data of this type is important in the design of remote sensors and in the interpretation of the sensor outputs. More significantly, the combined data[7] from simultaneous radar and radiometer measurements can be used to provide even more effective classification of terrain surfaces, and better estimates of surface characteristics such as roughness and dielectric constant, than either sensor alone.

REFERENCES

1. Moore, R.K. and D.S. Simonett, "Potential Research and Earth Resource Studies with Orbiting Radars: Results of Recent Studies," AIAA 4th Annual Meeting and Technical Display, No. 67-767, October 1967.
2. Dellwig, L.F., J.N. Kirk, and R.L. Walters, "The Potential of Low-Resolution Radar Imagery in Regional Geologic Studies," J. Geophs. Res., Vol. 71, No. 20, pp 4995-4998, 1966.
3. MacDonald, H.C., P.A. Brennan, and L.F. Dellwig, "Geologic Evaluation by Radar of NASA Sedimentary Test Site," IEEE Trans. of Geosci. Electronics, Vol. GE-5, No. 3, December 1967.
4. Dellwig, L.F., and R.K. Moore, "The Geological Value of Simultaneously Produced Like-and Cross-Polarized Radar Imagery," J. Geophys. Res., Vol 71, No. 14, pp. 3597-3601, July 1966.
5. Ladley, A.E., "Radiometry for Ice Detection" The Engineer's Digest (USCG), No. 154, p 34-38, January-February-March 1967.
6. Catoe, C., W. Nordberg, P. Thaddeus, and G. Ling, "Preliminary Results from Aircraft Flights of an Electrically Scanning Microwave Radiometer," NASA Rept. X-622-67-352, GSFC, August 1967.
7. Peake, W.H.,R.L. Riegler, and C. H. Schultz, "The Mutual Interpretation of Active and Passive Microwave Sensor Outputs," Proc. Fourth Symp. on Remote Sensing of Environment, Univ. of Michigan, pp. 771-777, April 1966.

8. Cosgriff, R.L., W.H. Peake, and R.C. Taylor, "Terrain Scattering Properties for Sensor System Design," Ohio State University Engineering Experiment Station Bulletin 181, Vol 29, No. 3, (Terrain Handbook II), 1960.

9. Peake, W.H., "Scattering from Rough Surfaces, Such as Terrain," Antenna & Scattering Theory: Recent Advances, Department of Electrical Engineering Short Course, 1966.

10. Weiner, G., "An 8.6mm CW Reflection Measuring System," Report 694-1, ElectroScience Laboratory, Department of Electrical Engineering, The Ohio State University, 31 October 1956; prepared under Contract AF 33(616)-3649, Wright Air Development Center, (AD 1186 38).

11. Barrick, D., "Normalization of Bistatic Radar Return," Report 1388-13, ElectroScience Laboratory, Department of Electrical Engineering, The Ohio State University, 15 January 1964; prepared under Grant No. NsG-213-61, National Aeronautics and Space Administration.

12. Peake, W.H., "Estimates of Bias Errors in Narrow Beam Microwave Systems," to be published.

13. Ott, R.H., "The Scattering by a Two-Dimensional Periodic Array of Plates," Technical Report 2148-2, ElectroScience Laboratory, Department of Electrical Engineering, The Ohio State University, 30 June 1966; prepared under contract AF 33(615)-3461, Air Force Avionics Laboratory, Wright-Patterson Air Force Base, Ohio (AD 486 777).

14. Munk, B.A., "Scattering by Periodic Arrays of Loaded Elements," Dissertation, to be published, August 1968.

15. Riegler, R.L., "Microwave Radiometric Temperatures of Terrain," Report 1093-2, ElectroScience Laboratory, Department of Electrical Engineering, The Ohio State University, 30 June 1966, prepared under Grant No. NsG-74-60, National Aeronautics and Space Administration.

16. Peake, W.H., "The Microwave Radiometer as a Remote Sensing Instrument, with Applications to Geology," Notes prepared for a Short Course on Geologic Remote Sensing, Stanford University, December 4-8, 1967.

17. Ewen, H.I., "State of the Art of Microwave and Millimeter Wave Radiometric Sensors " Int. Symp. on Electromagnetic Sensing of the Earth from Satellites, Miami Beach, Florida, Nov. 22-24, 1965.

18. Twomey, S., "The Application of Numerical Filtering to the Solution of Integral Equations Encountered in Indirect Sensing Measurements," J. Franklin Inst., 279(2), 95-109, 1965.

19. Iglesias, J., and W.B. Westphal, "Supplementary Dielectric Constant and Loss Measurements," Tech. Repot No. 203, Lab. for Insulation Research, Massachusetts Institute of Technology, January 1967.

20. Parkhomenko, E.I., Electrical Properties of Rocks, Plenum Press, 1967.

21. Interim Technical Report, 2440-1, ElectroScience Laboratory, Department of Electrical Engineering, The Ohio State University, 22 December 1967; prepared under Contract F33615-67-C-1663, Air Force Avionics Laboratory, Wright-Patterson Air Force Base,Ohio.

APPENDIX I

RADAR ANTENNA POWER PATTERNS

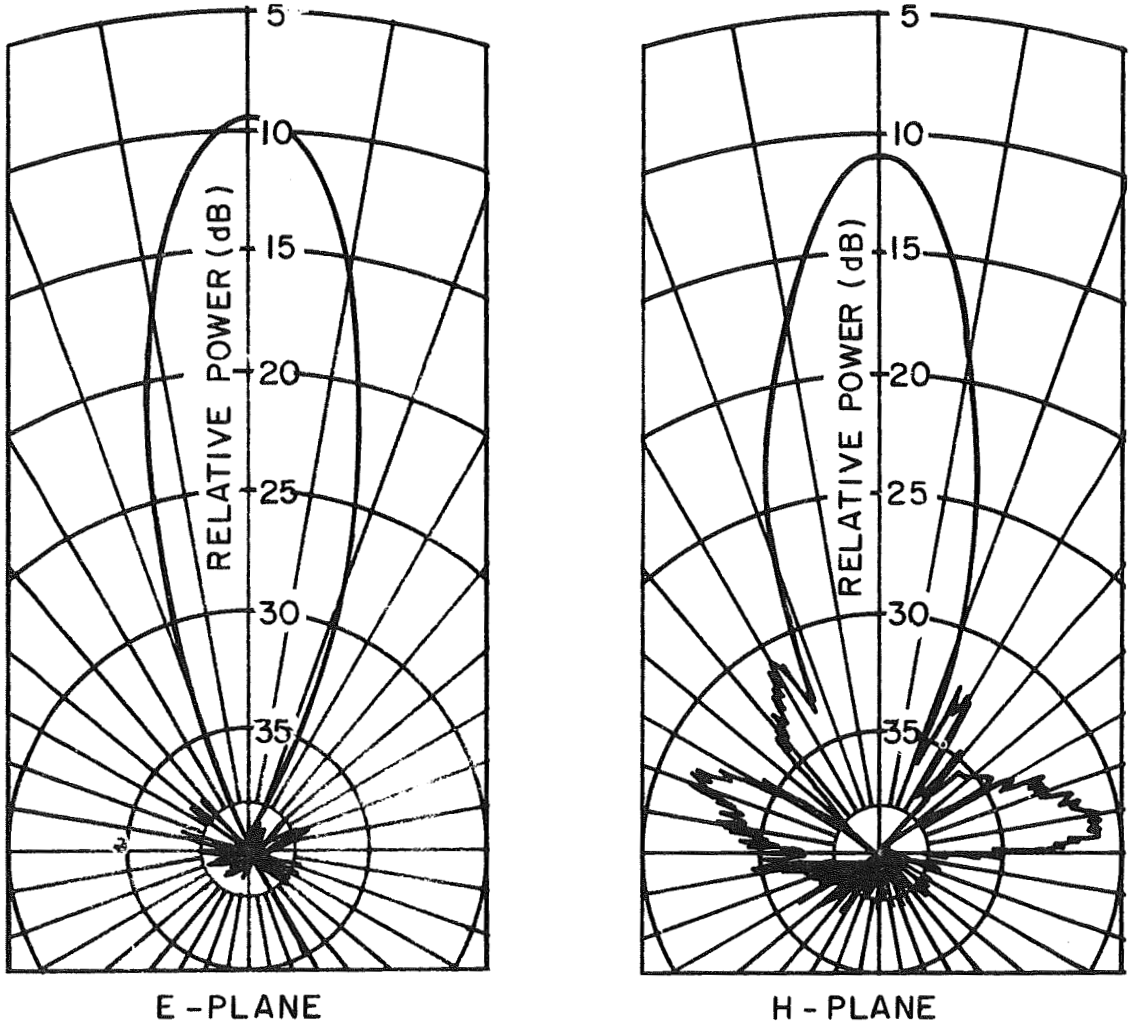

Fig. 40 . S-band radar antenna patterns (1.8 GHz).

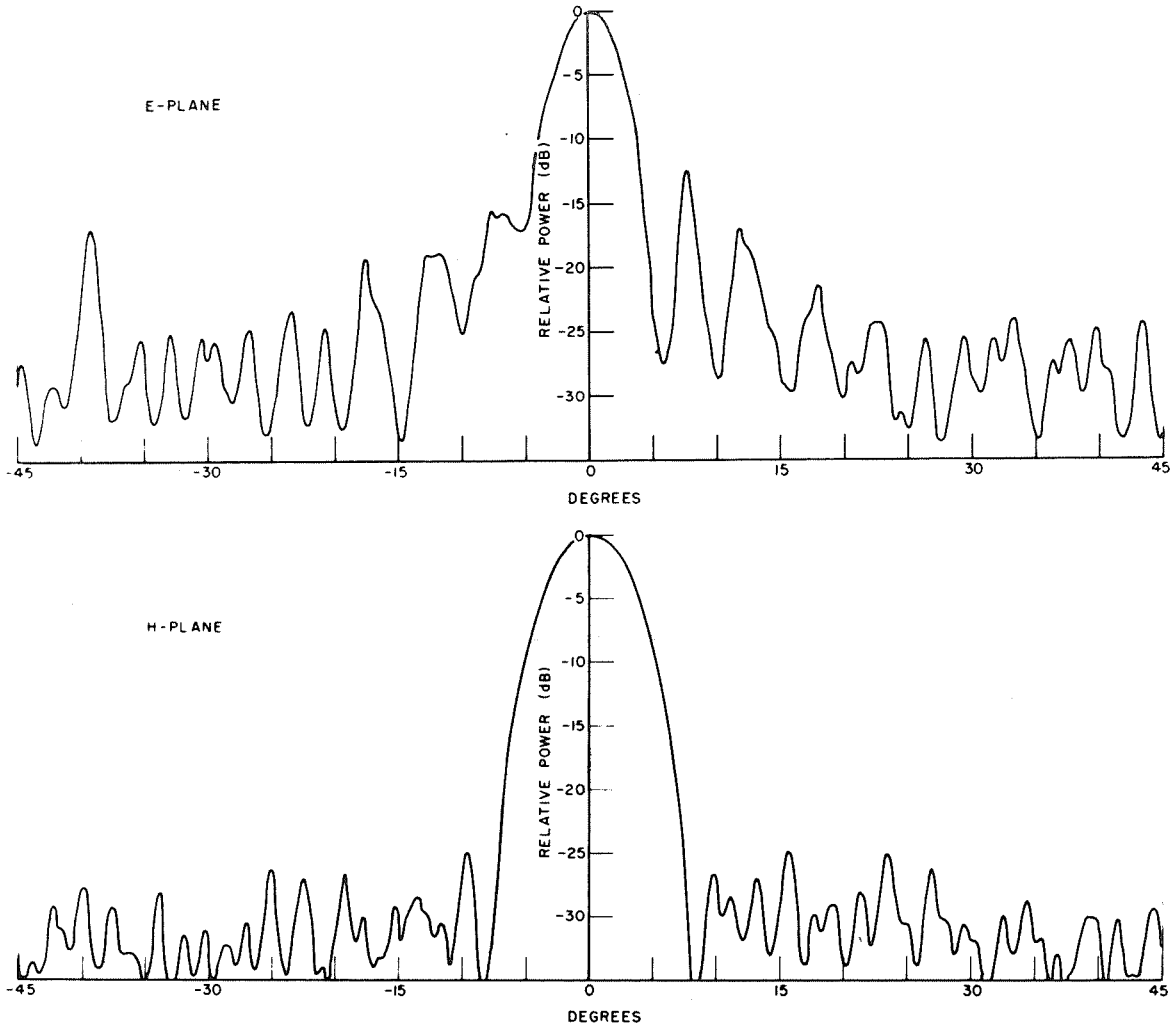

Fig. 41. X-band radar antenna patterns (10 GHz).

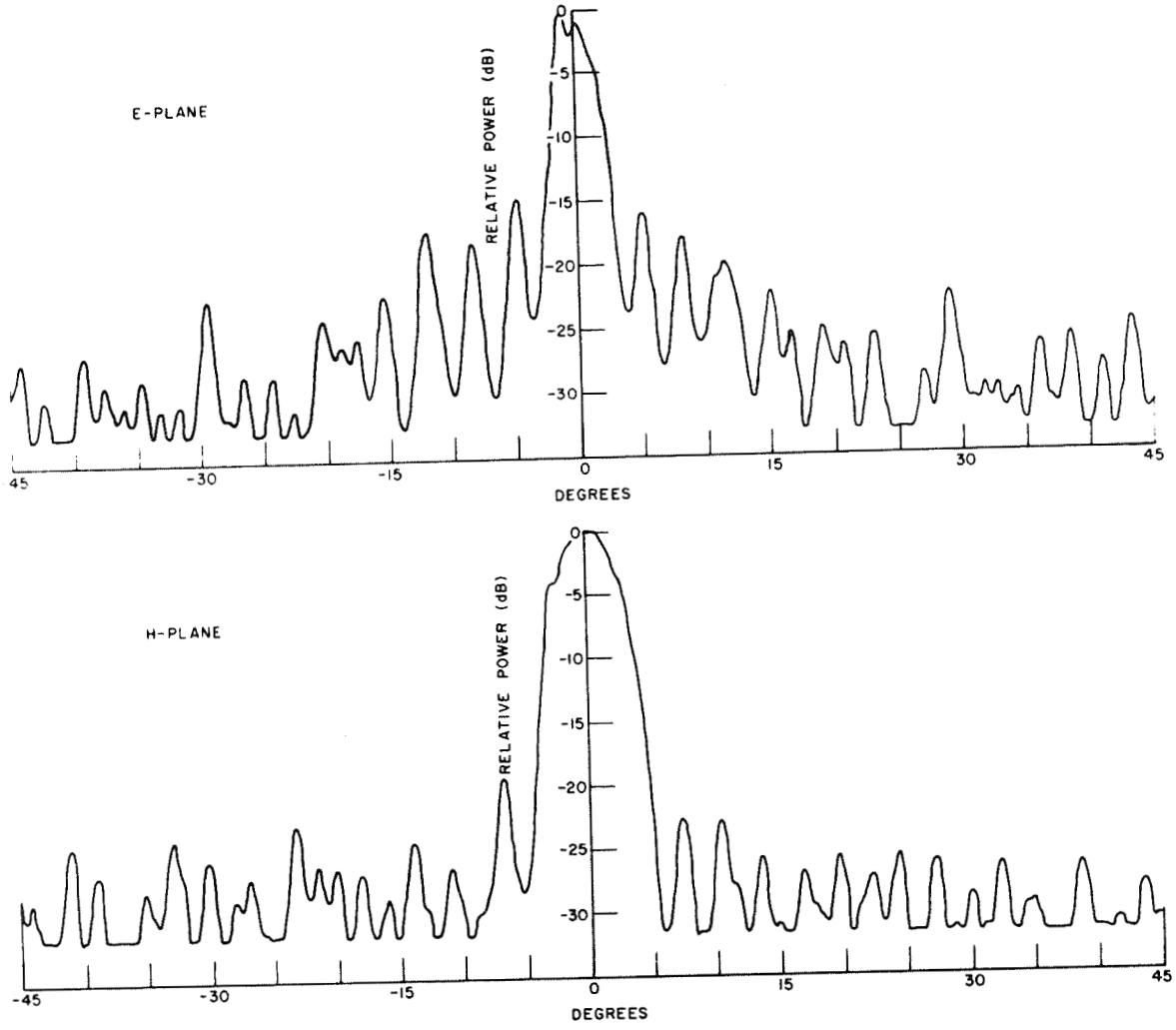

Fig. 42. K_u-band radar antenna patterns (15 GHz).

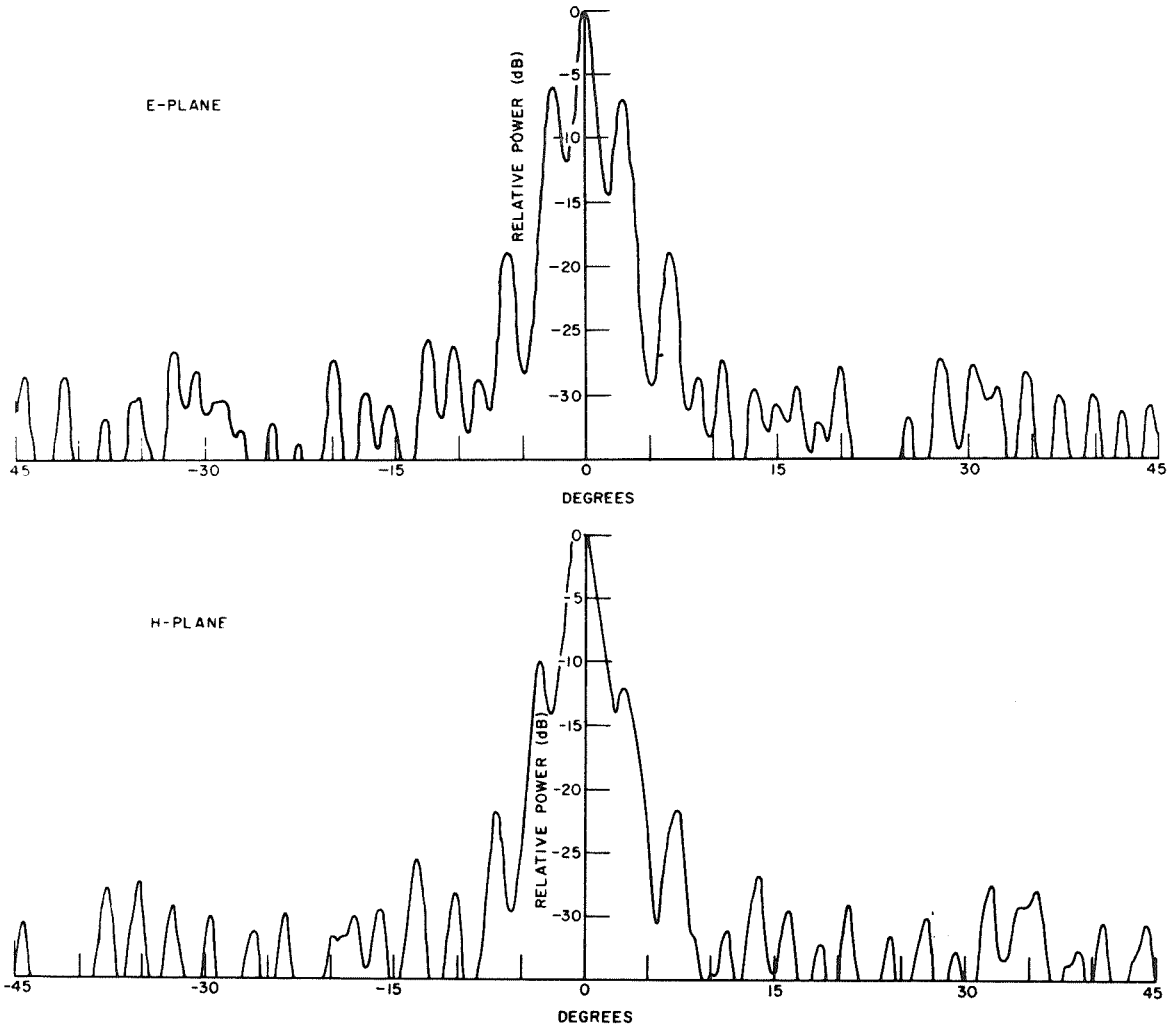

Fig. 43 . K_a-band radar antenna patterns (35 GHz).

APPENDIX II

RADIOMETER ANTENNA POWER PATTERNS[15]

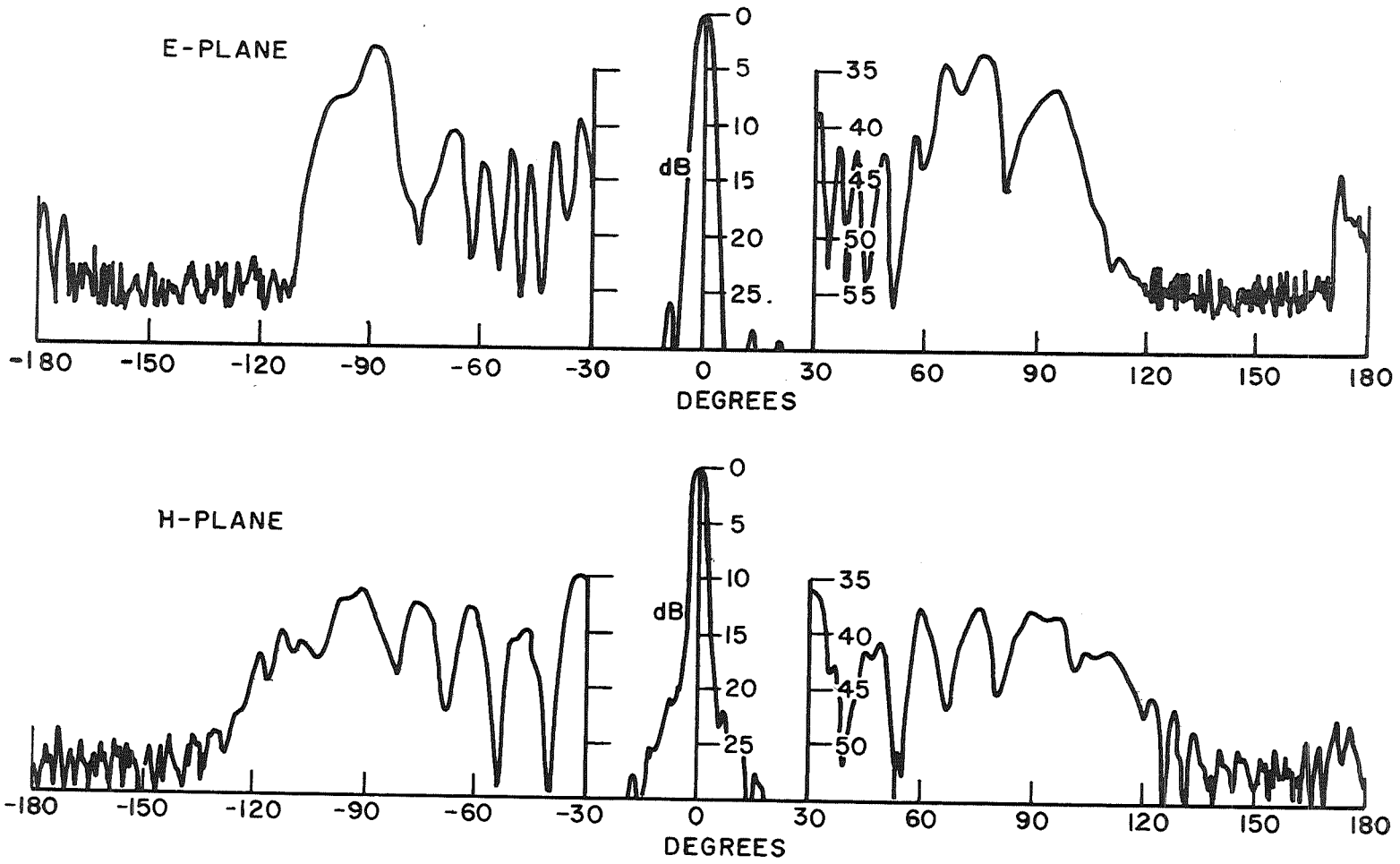

Fig. 44. X-band radiometer antenna patterns (10 GHz).

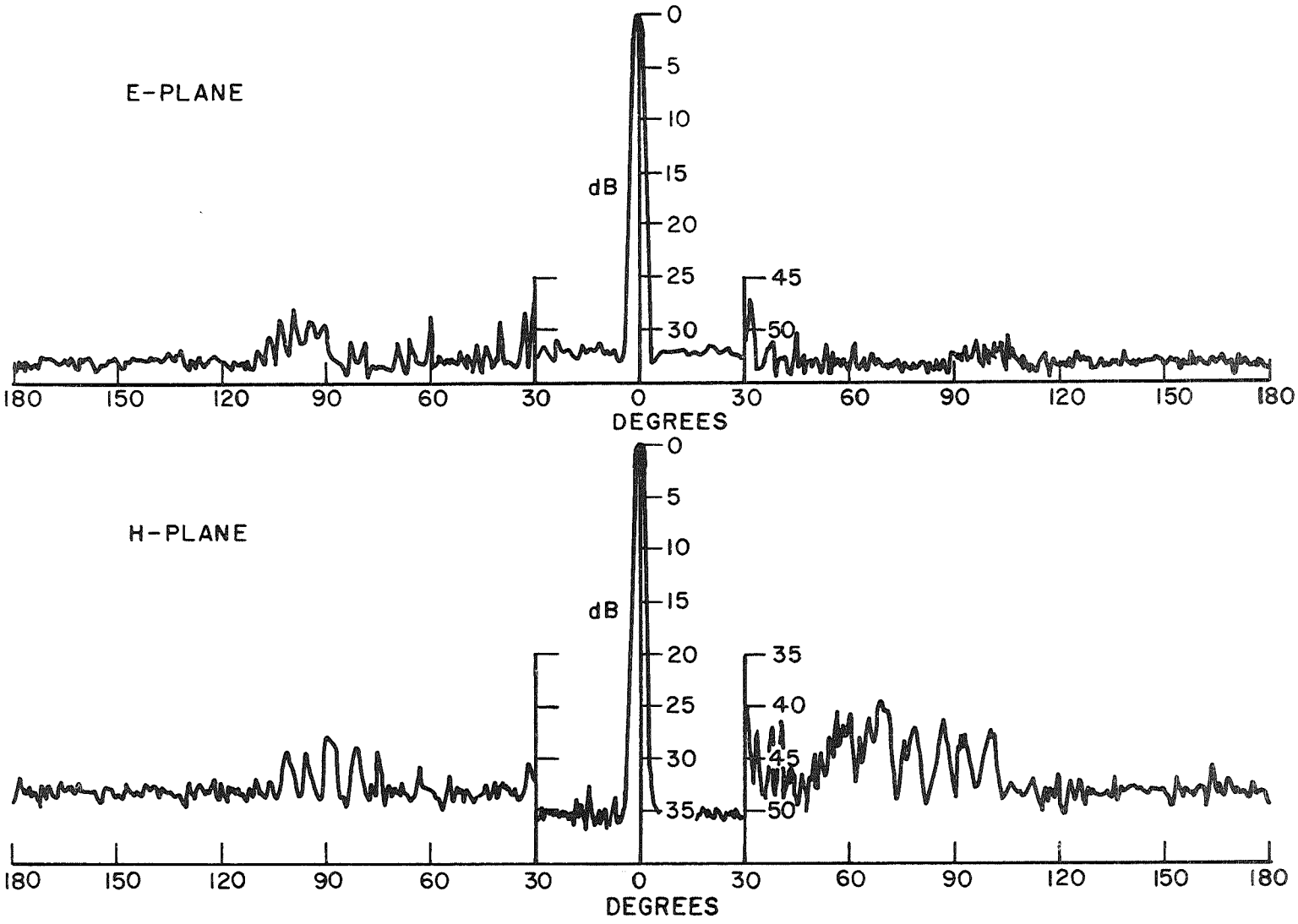

Fig. 45. K_a-band radiometer antenna patterns (35 GHz).

APPENDIX III

RADAR BACKSCATTERING COMPUTER PROGRAM

```
$EXECUTE        OSUSYS
$OSUSYS         RUN(1000,5000)
$SCATRAN        OBDECK,SLIST                                          MAIN0001
C              BACKSCATTERING PROGRAM FOR PROJECT 1903-
C              MAIN PROGRAM START-
C              -
               INTEGERS(SCAT,CUE,RUN,HRUN,VRUN,DATE,CRUN,BRUN,IDANT,)-
               BOOLEAN(PPLOT,GPLOT,FR)-
C              -
C              FORMATS-
C              -
F FORM1        (17X,I3,17X,L6)-
F GHD          (1H1,17X,Q*MEASURED BACKSCATTERING CROSS SECTION PER UNIT AR
               EA VS. INCIDENCE ANGLE FROM NORMAL *//13X,Q*DATA GROUP NUMBE
               R = *,I3,21X,8HTERRAIN ,2L6,9X,12HFREQUENCY = ,F7.3,10H GIGA
               HERTZ/5X,Q*DATE  *,L6/)-
F ABS            -
F ABSF               -
F ORD          GAMMA IN DECIBELS-
F FFREQ        FREQUENCY-
F FFREQ1       GHZ-
F ANGLE2       DEGREES-
F TTER         TERRAIN IDENTIFICATION-
F MARKH        HORIZONTAL POLARIZATION O -
F MARKV        VERTICAL POLARIZATION    +  -
F MARKC        CROSS POLARIZATION       X   -
F GEND         (/Q$END OF PLOT FOR GROUP NUMBER$,I4)-
F HEAD3        (/49X,21HVERTICAL POLARIZATION )-
F HEAD4        (/48X,23HHORIZONTAL POLARIZATION )-
F HEAD5        (/41X,19HCROSS POLARIZATION    ,Q* VERTICAL TRANSMITTER*)-
F HEAD6        (/40X,19HCROSS POLARIZATION  ,Q* HORIZONTAL TRANSMITTER*)-
F COLHD        (/11H RUN NUMBER,6X,  Q*                                *    ,22HABSO
               LUTE CROSS SECTION ,6X,25HCROSS SECTION IN DECIBELS,6X,17HGA
               MMA IN DECIBELS )-
F FRTIME       (/4X,41HINTEGRATION TIME FROM REFERENCE SPHERE =  ,F7.3,8H S
               ECONDS ,10X,Q*VOLTAGE*,F7.3,6H VOLTS,10X,Q*MULTIPLIER*,F4.1,
               /10X,Q*TIME/VOLT*,F10.5,10X,Q*INPUT*,F10.5,10X,Q*IN DB*,F10.
               5,10X,Q* FREQUENCY*,F5.1/)-
F FPLOT        (15X,Q*NO PLOTS REQUESTED* )-
F FFRUN        (1H+,49X,Q*FREQUENCY RUN AT CONSTANT ANGLE OF *,F10.2/)-
F DATA         (4X,L2,5X,I3,5X,F4.1,6X,F4.1,6X,F5.3,21X,F3.1)-
F FFN          (50X,Q* CONSTANT ANGLE OF*,F5.2,Q*DEGREES*)-
F AFM          (50X,Q*CONSTANT FREQUENCY OF *,F5.2,Q* GIGAHERTZ *)-
F DATB         (5X,I3,13X,F5.1,23X,F12.8,19X,F8.3,19X,F8.3)-
F FORM2        (13X,I3,4X,2L6,6X,L2,11X,F5.2,10X,L6/12X,F4.1,6X,F5.3,6X,
               F3.1,6X,F4.1,19X,L4)-
F FORM3        (12X,F4.1,6X,F5.3,6X,F3.1,6X,F4.1,19X,L4)-
C              -
C              DIMENSION STATEMENTS-
C              -
               DIMENSION(CRUN(25),CANGLE(25),CSIG(25),CLSIG(25),CLGSIG(25),
               BRUN(25),BANGLE(25),BSIG(25),BLSIG(25),BLGSIG(25))-
               DIMENSION(ID(2),ANT(4),HRUN(25),HANGLE(25),HSIG(25),HLSIG(25
               ),HLGSIG(25),VRUN(25),VANGLE(25),VSIG(25),VLSIG(25),VLGSIG(2
               5),ARRAY(44))-
C              -
C              FIRST DATA CARD CONTAINS ANTENNA BEAM WIDTHS CENTER TO 3DB.-
C              -
  START        CONTINUE-
               READ INPUT,7,((ANT(I),I=0,1,I.L.4))-
C              SECOND CARD  ...  NUMBER OF GROUPS AND REQUEST FOR NO PLOTS-
               PPLOT(=)0-
               READINPUT,FORM1,(NGROUP,IPLOTS)-
               PROVIDED (IPLOTS.NE.$ $),PPLOT(=),0.777777777777 -
```

```
                PROVIDED(PPLOT),TRANSFER(BEGIN)-
                CALLSUBROUTINE()=PLOTS,(ARRAY,44,0)-
  BEGIN         DOTHROUGH(END),K=1,1,K.LE.NGROUP-
                GPLOT(=)0-
                FR(=)0-
                READINPUT,FORM2,(NUMBER,ID(0),ID(1),NPLOTS,CONSTA,DATE,STIME
                      ,SVOLT,CCC,FRUN,SCAT)-
                PROVIDED(NPLOTS.NE.$ $),GPLOT(=).0.777777777777-
C               -
C               -
C               CARD IMAGES-
C               GROUP NUMBER NNN ID LLLLLLLLLLLL PLOT LL RUN ANGLE NNNNN DEG
                 DATE LLLLLL-
C               -
C               SPHERE TIME XX.X VOLT X.XXX MULT X.X FREQ XX.X GHZ S/V XXXX.
                XXX             -
C               -
                PROVIDED(CONSTA.NE.0.),FR(=).0.777777777777-
C               -
C               CALCULATE REFERENCE VOLTAGE-
C               -
                STV=CCC/SVOLT*STIME-
                VS=INT.(STV)-
C               -
C               GROUP HEADING WRITE OUT -
                WRITENO HEADING,GHD,(NUMBER,ID(0),ID(1),FRUN,DATE)-
                PROVIDED(PPLOT.OR.GPLOT),WRITEOUTPUT,FPLOT-
                PROVIDED(FR),WRITEOUTPUT,FFRUN,(CONSTA)-
                DBVS=20.*LOG.(VS)-
                WRITEOUTPUT,FRTIME,(STIME,SVOLT,CCC,STV,VS,DBVS,FRUN)-
C               -
C               FREQUENCY OR ANGLE RUN-
                TRANSFER(SPEC) PROVIDED( FR)-
C               -
C               FORMAT MODIFICATION-
                COLHD(4)(=)$BACKSC$-
                COLHD(5)(=)$ATTERI$-
                COLHD(6)(=)$NG ANG$-
                COLHD(7)(=)$LE     $-
C               -
C               THE FOLLOWING IS FOR AN ANGLE RUN-
C               -
C               SELECT ANTENNA-
                I=IDANT.(FRUN)-
                L=0-
                M=0-
                MA=0-
                J=0-
  READON        READINPUT,DATA,(CUE,RUN,ANGLE,TIME,VOLT,CMULT)-
C               -
C               CARD IMAGE-
C               -
C               POL LL RUN NNN ANG XX.X TIME XX.X VOLT X.XXX S/V XXXX.XXX N
                MULT X.X LLL-
C               -
C               GROUP END SIGNIFIED BY TIME=0.-
                PROVIDED(TIME.E.0.),TRANSFER(OUT)-
                TV=CMULT/VOLT*TIME-
                FACTOR=TABCAL.(ANGLE)*ANT(I)/4.1209*ANT(I)-
C               SELECTION OF PROPER STORAGE ARRAY-
                TRANSFER(VERT,VERT,HORO)PROVIDED(CUE)-
C               -
C               HORIZONTAL INPUTS-
```

```
  HORO      TRANSFER(HH,HH,HV)PROVIDED(CUE-$HH$)-
  HH        HRUN(L)=RUN-
            HANGLE(L)=ANGLE-
            CALLSUBROUTINE(HSIG(L),HLSIG(L),HLGSIG(L))=CAL.(ANGLE,INT.(
            TV),VS,FACTOR)-
            L=L+1-
            TRANSFER(READON)-
  VERT      TRANSFER(VV,VH,VH)PROVIDED(CUE-$VH$)-
  VV        VRUN(J)=RUN-
            VANGLE(J)=ANGLE-
            CALLSUBROUTINE(VSIG(J),VLSIG(J),VLGSIG(J))=CAL.(ANGLE,INT.(
            TV),VS,FACTOR)-
            J=J+1-
            TRANSFER(READON)-
C           CROSS POLARIZATION ANGLE RUN-
C           -
C           VERTICAL TRANSMITTER-
  VH        CRUN(M)=RUN-
            CANGLE(M)=ANGLE-
            CALLSUBROUTINE(CSIG(M),CLSIG(M),CLGSIG(M))=CAL.(ANGLE,INT.(
            TV),VS,FACTOR)-
            M=M+1-
            TRANSFER(READON)-
  HV        BRUN(MA)=RUN-
            BANGLE(MA)=ANGLE-
            CALLSUBROUTINE(BSIG(MA),BLSIG(MA),BLGSIG(MA))=CAL.(ANGLE,INT
            .(TV),VS,FACTOR)-
            MA=MA+1-
            TRANSFER(READON)-
C           -
C           -
C           THIS PART FOR FREQUENCY RUN-
  SPEC      ANGLE=CONSTA-
            I=IDANT.(FRUN)-
C           -
C           FORMAT MODIFICATION-
            COLHD(4)(=)$    RUN$-
            COLHD(5)(=)$ FREQU$-
            COLHD(6)(=)$ENCY   $-
            COLHD(7)(=)$   $-
C           -
C           SCATTER REQUEST-
            PROVIDED(SCAT.NE.$ $),TRANSFER(FRSCAT)-
            TAB=TABCAL.(ANGLE)-
            J=0-
            L=0-
            M=0-
            MA=0-
C           -
C           CARD IMAGE-
C           -
C           POL LL RUN NNN FRQ XX.X TIME XX.X VOLT X.XXX S/V XXXX.XXX N
            MULT X.X LLL-
C           -
  RDF       READINPUT,DATA,(CUE,RUN,FREQU,TIME,VOLT,CMULT)-
            PROVIDED(TIME.E.0.),TRANSFER(RDF2)-
            TV=CMULT/VOLT*TIME          -
            FACTOR=TAB             *ANT(I)/4.1209*ANT(I)-
C           -
C           THIS PROGRAM HAS SELECTION OF EITHER POLARIZATION-
            TRANSFER(VF,VF,HF)PROVIDED(CUE)-
C           -
C           HORIZONTAL FREQUENCY RUN-
  HF        TRANSFER(HHF,HHF,HVF)PROVIDED(CUE-$HH$)-
```

```
  HHF       HRUN(L)=RUN-
            HANGLE(L)=FREQU-
            CALLSUBROUTINE(HSIG(L)*HLSIG(L)*HLGSIG(L))=CAL*(ANGLE*INT*(
            TV)*VS*FACTOR)-
            L=L+1-
            TRANSFER(RDF)-
  VF        TRANSFER(VVF*VVF*VHF)PROVIDED(CUE-$VV      $)-
 VVF        VRUN(J)=RUN-
C           -
C           VERTICAL POLARIZATION FREQUENCY RUN-
            VANGLE(J)=FREQU-
            CALLSUBROUTINE(VSIG(J)*VLSIG(J)*VLGSIG(J))=CAL*(ANGLE*INT*(
            TV)*VS*FACTOR)-
            J=J+1-
            TRANSFER(RDF)-
C           -
C           CROSS POLARIZATION FREQUENCY RUN-
C           -
C           VERTICAL TRANSMITTER-
  VHF       CRUN(M)=RUN-
            CANGLE(M)=FREQU-
            CALLSUBROUTINE(CSIG(M)*CLSIG(M)*CLGSIG(M))=CAL*(ANGLE*INT*(
            TV)*VS*FACTOR)-
            M=M+1-
            TRANSFER(RDF)-
C           -
C           CROSS POLARIZATION  HORIZONTAL TRANSMITTER-
  HVF       BRUN(MA)=RUN-
            BANGLE(MA)=FREQU-
            CALLSUBROUTINE(BSIG(MA)*BLSIG(MA)*BLGSIG(MA))=CAL*(ANGLE*INT
            *(TV)*VS*FACTOR)-
            MA=MA+1-
            TRANSFER(RDF)-
C           -
C           -
C           PLOTTING AND WRITEOUTPUT OF DATA CALCULATED-
  OUT       PROVIDED(J*E*0)*TRANSFER(HWRITE)-
            WRITENOHEADING*HEAD3-
            WRITENOHEADING*COLHD-
            WRITENOHEADING*DATB*((VRUN(JR)*VANGLE(JR)*VSIG(JR)*VLSIG(JR)
            *VLGSIG(JR)*JR=0*1*JR*L*J))-
  HWRITE    PROVIDED(L*E*0)*TRANSFER(CWRITE)-
            WRITENOHEADING*HEAD4-
            WRITENOHEADING*COLHD-
            WRITENOHEADING*DATB*((HRUN(JR)*HANGLE(JR)*HSIG(JR)*HLSIG(JR)
            *HLGSIG(JR)*JR=0*1*JR*L*L))-
  CWRITE    PROVIDED(M*E*0)*TRANSFER(BWRITE)-
            WRITENOHEADING*HEAD5-
            WRITENOHEADING*COLHD-
            WRITENOHEADING*DATB*((CRUN(JR)*CANGLE(JR)*CSIG(JR)*CLSIG(JR)
            *CLGSIG(JR)*JR=0*1*JR*L*M))-
  BWRITE    PROVIDED(MA*E*0)*TRANSFER(GOON)-
            WRITENOHEADING*HEAD6-
            WRITENOHEADING*COLHD-
            WRITENOHEADING*DATB*((BRUN(JR)*BANGLE(JR)*BSIG(JR)*BLSIG(JR)
            *BLGSIG(JR)*JR=0*1*JR*L*MA))-
  GOON      PROVIDED(GPLOT*OR*PPLOT)*TRANSFER(END)-
C           -
C           PLOTTING COMMANDS FOR GRAPHS FOLLOW-
C           -
C           HORIZONTAL AXIS-
            FNUM=NUMBER-
            PROVIDED(FR)*TRANSFER(AX2)-
            CALLSUBROUTINE()=AXIS*(0*,*0*,*ABS*-1*,*-4*5*0*,*0*,*20*,*5)-
```

```
                TRANSFER(AXX)-
   AX2          CALLSUBROUTINE()=AXIS.(0..0..ABSF.-2.-4.5.0..0..8...5)-
   AXX          FNUM=NUMBER-
                CALLSUBROUTINE()=SYMBOL.(1..1.75..14.$GROUP$.0..5)-
                CALLSUBROUTINE()=NUMBER.(1.7.1.75..14.FNUM.0..-1)-
                PROVIDED(FR).TRANSFER(LABEL1)-
                CALLSUBROUTINE()=SYMBOL.(1..1.5..14.FFREQ.0..11)-
                CALLSUBROUTINE()=NUMBER.(2.45.1.5..14.FRUN.0..1)-
                CALLSUBROUTINE()=SYMBOL.(3.52.1.5..14.FFREQ1.0..3)-
                TRANSFER(LABEL2)-
   LABEL1       CALLSUBROUTINE()=SYMBOL.(1..1.5..14.$ANGLE $.0..6)-
                CALLSUBROUTINE()=NUMBER.(1.8.1.5..14.ANGLE.0..1)-
                CALLSUBROUTINE()=SYMBOL.(2.6.1.5..14.ANGLE2.0..8)-
   LABEL2       CALLSUBROUTINE()=SYMBOL.(1..1.25..14.ID.0..12)-
                CALLSUBROUTINE()=SYMBOL.(1..1...14.$DATE$.0..4)-
                CALLSUBROUTINE()=SYMBOL.(1.7.1...14.DATE.0..6)-
                CHG=20.-
                PROVIDED(FR).CHG=8.-
C               -
C               VERTICAL AXIS-
                CALLSUBROUTINE()=AXIS.(0..0..ORD.-0..-10..270..5..-5..1.)-
                CALLSUBROUTINE()=LINE.(VANGLE.0..CHG.VLGSIG.5..5..J.1.3)-
                CALLSUBROUTINE()=LINE.(HANGLE.0..CHG.HLGSIG.5..5..L.1.1)-
                CALLSUBROUTINE()=LINE.(CANGLE.0..CHG.CLGSIG.5..5..M.1.4)-
                CALLSUBROUTINE()=LINE.(BANGLE.0..CHG.BLGSIG.5..5..MA.1.12) -
                CALLSUBROUTINE()=PLOT.(8..0..-3)-
   END          CONTINUE-
                CALLSUBROUTINE()=PLOTE.()-
                CALLSUBROUTINE()=ENDJOB.()-
   FRSCAT       CONTINUE-
                WRITEOUTPUT.ERR-
F ERR           (Q*        NO SCATTER ROUTINE IN PROGRAM JOB FORCED OFF BY PR
                OGRAM*///)-
                CALLSUBROUTINE()=ENDUMP.()-
   RDF2         READINPUT.FORM3.(STIME.SVOLT.CCC.FRUN.SCAT)-
                I=IDANT.(FRUN)-
C               END OF GROUP SIGNIFIED BY TIME=0.-
                PROVIDED(STIME.E.0.).TRANSFER(OUT)-
                STV=CCC/SVOLT*STIME-
                VS=INT.(STV)-
                DBVS=20.*LOG.(VS)-
                WRITEOUTPUT.FRTIME.(STIME.SVOLT.CCC.STV.VS.DBVS.FRUN)-
                TRANSFER(RDF)-
                ENDPROGRAM(START)-
$FAP                                                            TABC0001
        COUNT   50
*       SUBROUTINE TO DETERMINE TAB FOR A GIVEN ANGLE
        ENTRY   TABCAL
        REM     SCATRAN CALLING SEQUENCE
        REM     CALLSUBROUTINE(TABA)=TABCAL.(ANGLE)-
        REM     THE RESULT IS ALSO IN THE AC ON RETURN
TAB     DEC     .0030216
        DEC     .0030698
        DEC     .0032242
        DEC     .0035130
        DEC     .0039995
        DEC     .0048216
        DEC     .0063145
        DEC     .0093387
        DEC     .0151546
        DEC     1.0
PART    PZE
I       PZE
IANG    PZE
```

```
TABCAL  SXA     IR1,1           SAVE IR1
        SXA     IR4,4                IR4
        CAL*    1,4             IANG=ANGLE
        TSX     $FLFX,4
        STO     IANG
        XCA                     PUT DIVIDEND INTO MQ
        PXA     0,0             CLEAR AC
        DVP     =10             I=IANG/10
        XCA                     GET ANSWER BACK INTO AC
        PAC     0,1             PUT AD(AC) INTO IR1
        CLA     IANG            PART=(ANGLE-IANG)/10.
        TSX     $FXFI,4
        CHS
IR4     AXT     0,4             RESTORE IR4
        FAD*    1,4
        FDP     =10.
        STQ     PART
        CLA     TAB+1,1
        FSB     TAB,1
        XCA
        FMP     PART
        FAD     TAB,1           ((TAB+1)-TAB)*PART + TAB
IR1     AXT     **,1            RESTORE IR1
        STO*    2,4             STORE ANSWER
        TRA     3,4             RETURN TO CALLING PROGRAM
        END
$FAP                                                            CAL 0001
        COUNT   80
*THIS SUBROUTINE DOES THE CALCULATION OF THE INPUT VOLTAGE IN DB.
*  PROPER SCATRAN CALLING SEQUENCE
*  CALL SUBROUTINE(VSIG,VLSIG,VLGSIG)=CAL.(ANGLE,V,REFV,FAC)-
        ENTRY   TTT
        ENTRY   CAL
TT      DEC     .000816691371672
        DEC     .000928058376949
        DEC     .000928058376949
        DEC     .000928058376949
TEMP    PZE
FAC     DEC     .01745329               DEG TO RADIAN CONSTANT
VL      PZE
10A     DEC     10.
CAL     SXA     IR4,4           SAVE IR4
        CLA*    2,4             TEMP=V/REFV
        FDP*    3,4
        STQ     TEMP
        FMP     TEMP
        SXA     XR2,2     SAVE IR2
TTT     AXC     **,2       PLACE I FROM IDANT. IN IR2
        FDP*    4,4             VSIG=(V/REFV).P.2/FAC*TT
        FMP     TT,2
XR2     AXT     **,2            RESTORE IR2
        STO*    5,4
        STO     TEMP
        TSX     $FLOG1,4
        PZE     TEMP
        PZE     TEMP
        XCA
        FMP     10A             VL=10.*LOG(VSIG)
        STO     VL
IR4     AXT     **,4
        STO*    6,4
        LDQ     FAC             VLGSIG=VL-10. LOG(COS(ANGLE*PI/180))
        FMP*    1,4
        STO     TEMP
```

```
        TSX     $FCOS1,4
        PZE     TEMP
        PZE     TEMP
        TSX     $FLOG1,4
        PZE     TEMP
        PZE     TEMP
        XCA
        FMP     10A
        CHS
        FAD     VL
        LXA     IR4,4           RESTORE IR4
        STO*    7,4
        TRA     8,4
        END
$FAP                                                            IDAN0001
        COUNT   60
* ROUTINE TO DETERMINE ANTENNA USED
*  SCATRAN CALLING SEQUENCE
*     CALL FUNCTION (I)=IDANT.(FREQ)
        ENTRY   IDANT
IDANT   SXA     IR1,1           SAVE REGISTER
        AXT     0,1
        CLA*    1,4
        CAS     =11.            FREQ GREATER THAN 11.
        TRA     HIGH            YES
        TRA     HIGH            YES
        CAS     =1.9            NO  FREQ GREATER THAN 1.9
        TXI     EXIT,1,1        YES
        TXI     EXIT,1,1        YES
        TXI     EXIT,1,0        NO
HIGH    CAS     =16.            FREQ GREATER THAN 16.
        TXI     EXIT,1,3        YES
        TXI     EXIT,1,3        YES
        TXI     EXIT,1,2        NO
EXIT    PXA     0,1             I=IR1
        STO*    2,4
IR1     AXT     **,1            RESTORE IR1
        STA*    $TTT            STORE FOR USE BY OTHER SUBROUTINE
        TRA     3,4
        END
$FAP                                                            INT 0001
        COUNT   100
*       ROUTINE TO SIMULATE INTEGRATORS
*       USING FOUR  STRAIGHT LINE APPROXIMATIONS
        ENTRY   INT
*       CALLED BY    (VOLTIN)=INT.(TPV)
C1.     DEC     2.3
C2.     DEC     1.265
C3.     DEC     .809
E0.     DEC     .95
E1.     DEC     .8846
E2.     DEC     .626
E3.     DEC     .5221
T       PZE
CA      PZE
EA      PZE
1A      DEC     1.
10A     DEC     10.
75A     DEC     75.
INT     SXA     A,4             SAVE IR4
        CLA*    1,4             GET ARGUMENT
        STO     T               PUT IT IN T
        CAS     10A             COMPARE T AND 10
        TRA     A.              IF T GREATER
```

```
         TRA     A.                  EQUAL
         CAS     1A                COMPARE TO 1
         TRA     B.                IF GREATER
         TRA     B.                   EQUAL
         CLA     C1.                  LESS
         STO     CA
         CLS     E0.
         STO     EA
         TRA     PLUG
B.       CLA     C1.
         STO     CA
         CLS     E1.
         STO     EA
         TRA     PLUG
A.       CAS     75A               COMPARE TO 75
         TRA     D.                IF GREATER
         TRA     D.                   EQUAL
         CLA     C2.                  LESS
         STO     CA
         CLS     E2.
         STO     EA
         TRA     PLUG
D.       CLA     C3.
         STO     CA
         CLS     E3.
         STO     EA
PLUG     TSX     $FLOG1.4
         PZE     T
         PZE     T
         XCA
         FMP     EA
         STO     EA
         TSX     $FEXPT1.4         TAKE ANTILOG
         PZE     EA
         PZE     T
         XCA
         FMP     CA
 A       AXT     **.4              RESTORE IR4
         STO*    2.4
         TRA     3.4
         END
$DATA
  6.0      2.6          1.88        1.000
NO. OF GROUPS     163 PLOTS REQUESTED
```

APPENDIX IV

RADIOMETER COMPUTER PROGRAM FOR CONVERSION OF VOLTAGES TO ANTENNA TEMPERATURES

```
C:   RADIOMETER PROGRAM FOR
C:   CONVERSION OF VOLTAGES TO ANTENNA TEMPERATURES
C:   T=ANTENNA TEMPERATURE
C:   TA=THERMAL TEMPERATURE OF ANTENNA DEG. K
C:   TB=THERMAL TEMPERATURE OF BOX, DEG. K
C:   TO=THERMAL TEMPERATURE OF OVEN, 358.0 DEG. K
C:   V=OUTPUT VOLTAGE WITH ANTENNA
C:   V1=OUTPUT VOLTAGE WITH AMBIENT LOAD (20 DB ATTEN.)
C:   V2=OUTPUT VOLTAGE WITH OVEN LOAD  (0 DB ATTEN.)
C:   ANG=ANGLES WITH RESPECT TO NADIR
C:   A1=ANTENNA FEED LOSS
C:   A21=ATTENUATOR MAXIMUM LOSS (20 DB SETTING)
C:   A22=ATTENUATOR INSERTION LOSS (0 DB SETTING)
C:   FREQ=RADIOMETER FREQUENCY
DISPLAY ["ENTER FREQUENCY IN GHZ"]
ACCEPT[FREQ]
DISPLAY["ENTER TEMPERATURE OF ANTENNA IN DEG. K"]
ACCEPT[TA]
DISPLAY ["ENTER TEMPERATURE OF BOX IN DEG. K"]
ACCEPT [TB ]
DISPLAY ["ENTER VOLTAGE WITH AMBIENT LOAD"]
ACCEPT [V1]
DISPLAY ["ENTER VOLTAGE WITH OVEN LOAD"]
ACCEPT [V2]
IF (12.0-FREQ) 1,2,2
1 A1=0.8854
  A21=0.01
  A22=0.9465
GO TO 3
2A1=0.975
A21=0.01
A22=0.955
3 T2=(TB-(1.0-A1)*TA)/A1
TO=358.0
T3=(TO-TB)/A1
T4=A21*T3
T5=T3*(A21-A22)
T6=T2+T4
V3=V1-V2
DIMENSION ANG(50),V(50),T(50)
DISPLAY ["ENTER NUMBER OF DATA POINTS"]
ACCEPT [N]
DISPLAY ["ENTER ANGLES AND VOLTAGES"]
```

```
ACCEPT  (ANG(I),V(I), I=1,N)
DISPLAY ["ANGLE FROM NADIR", "ANTENNA TEMPERATURE"]
DO 4 I=1,N
T(I)=T6+T5*(V(I)-V1)/V3
4 DISPLAY [ANG(I), T(I)]
END
```

APPENDIX V

RADIOMETER COMPUTER PROGRAM FOR BRIGHTNESS TEMPERATURE INVERSION

```
$EXECUTE        OSUSYS
$OSUSYS         RUN(100,500)
$SCATRAN        OBJDECK,SLIST
C               SOLUTION OF INTEGRAL EQUATION TO FIND RAY TEMP.  -
  A0            TRANSFER(AL,AL,AH)PROVIDED(COSTH)-
  AL            TAVE=TEMP(1)-
                TRANSFER(S45)-
  AH            TAVE=TEMP(1)-
                TRANSFER(S45)-
                DIMENSION(DELT(220,NNN),TEMPR(220,NNN),ANGLE(50))-
                DIMENSION(THETP(300),FPNU(300),TEMP(50),TALS0(50),TANT(50))-
                LITERALS(SINE,0.  ,.173648178,.342020433,.5,.64278761,
                .766044443,.866025404,.939692621,.984807753,1.,
                .984807753,.939692621,.866025404,.766044443,.64278761,.5,
                .342020433,.173648178,0.,-.173648178,-.342020433,-.5,
                -.64278761,-.766044443,-.866025404,-.939692621,
                -.984807753,-1.,-.984807753,-.939692621,-.866025404,
                -.766044443,
                -.64278761,-.5,-.342020433,-.173648178,0.)-
  SA            READINPUT,6,(DENOM)-
                ITERMX=3-
                FM2(25)(=)ITERMX-
                ZYR(3)(=)ITERMX-
                READINPUT,8,(NN)-
                NNN=5-
                LITERALS(CF,.01745329)-
                DIMENSION(SINE(40))-
                BOOLEAN(TEST)-
F FMA           (I8)-
                DOTHROUGH(LOOPX),I=0,1,I.L.NN-
                READINPUT,Y,(THETP(I),PWR)-
                THETPR=THETP(I)*CF-
C               STORE SINE AND COSINE VALUES OF ANTENNA PATTERNS-
                DIMENSION(STHETP(300),CTHETP(300))-
                STHETP(I)=SIN.(THETPR)-
                CTHETP(I)=COS.(THETPR)-
 LOOPX          FPNU(I)=EXP10.(-PWR/10.)-
F Y             (2E16.8)-
                READINPUT,8,(JJ)-
                DOTHROUGH(S15),NSETS=1,1,NSETS.LE.JJ-
                READINPUT,FM1,(ITA,ITB,ITC,ITD,ITE,FREQ,ITF,ITG)-
                WRITEOUTPUT,FM2,(ITA,ITB,ITC,ITD,ITE,FREQ,ITF,ITG,(I,I,I=1,
                1,I.LE.ITERMX))-
F FM1           (5L6,F10.5,2L6)-
F FM2           (Q*1 TERRAIN *,2L6,//Q*  LOCATION *,2L6,10X,Q*DATE *,L6//
                Q*  FREQUENCY *,F10.1,Q* GHZ *,10X,2L6,Q* POLARIZATION*//
                Q* THETA*,11T,Q*TALS0*,21T,          (Q*DELTA T*, 11,2X,Q*TEM
                P*,11,5X))-
                ANG=0.  -
                DOTHROUGH(S10),III=1,1,ANG .L.180.-
                READINPUT,Y,(ANG,TEMP(III))-
                ANGL=ANG *CF-
                DIMENSION(CANGL(50),SANGL(50))-
                CANGL(III)=COS.(ANGL)-
                SANGL(III)=SIN.(ANGL)-
  S10           TALS0(III)=TEMP(III)-
                DOTHROUGH(S25),ITER=1,1,ITER.LE.ITERMX-
                DO THROUGH(S35),THETO=0.,10.,THETO.LE.180.-
                SUMAR=0.-
                THORA=THETO*CF-
                U=SIN.(THORA)-
                V=COS.(THORA)-
                DOTHROUGH(S40),N=1,1,N.L .NN-
                AREA=0.-
```

```
                COSTP=CTHETP(N)*V-
                Z=STHETP(N)-
                SING=U*Z-
                AREAP=FPNU(N)*Z*10.*CF*(THETP(N)-THETP(N-1))*CF-
                INTEGER$(PHI)-
                DOTHROUGH(S45),PHI=0.1,PHI.LE.35-
                COSTH=COSTP-SINE(PHI)    *SING-
                PROVIDED(.ABS.COSTH.LE.1.),TRANSFER(AD)-
                COTTH=COSTH/SQRT.(1.-COSTH*COSTH)-
                THDEG=FATAN2.(1.,COTTH)/CF-
                ITHET=THDEG-
                ITHLO=(ITHET/10)*10-
                I=(ITHLO/10)+1-
                THLO=ITHLO-
                TAVE=TEMP(I)+((THDEG-THLO)/10.)*(TEMP(I+1)-TEMP(I))-
    S45         AREA=AREA+TAVE*AREAP-
    S40         SUMAR=SUMAR+AREA-
                ITHETO=THETO-
                I=ITHETO/10+1-
    S35         TANT(I)=SUMAR/DENOM-
                DO THROUGH(S5),I=1,1,I.LE.19-
                DELTEM=TALSO(I)-TANT(I)-
                PROVIDED(.ABS.DELTEM.GE.30.),TEST(=).0.//////////-
                TEMP(I)=TEMP(I)+DELTEM-
                DELT(I,ITER)=DELTEM-
    S5          TEMPR(I,ITER)=TEMP(I)-
                PROVIDED(TEST),TRANSFER(OUTA)-
    S25         CONTINUE-
F   ZYR         (F5.3,5X,F5.1,5X,          (F7.1,F8.1,5X))-
    OUTA        DOTHROUGH(S99),I=1,1,I.L.20-
                THETA=10*(I-1)-
    S99         WRITEOUTPUT,ZYR,   (THETA    ,TALSO(I),(DELT(I,J),TEMPR(I,J),J
                =1,1,J.LE.ITERMX))-
    S15         CONTINUE-
                CALLSUBROUTINE()=ENDJOB.()-
                ENDPROGRAM(SA)-
```

ACKNOWLEDGMENTS

The author wishes to thank Dr. W.H. Peake for his contributions and guidance, both during the development of the facility and in the preparation of this report, and Mr. B.A. Munk and Mr. R.L. Riegler, whose earlier work provided a basis for the system development presented here. The assistance of Mr. Richard Grimes in making the terrain measurements is gratefully acknowledged.